

Aus dem Institut für Klinische Neuroimmunologie
der Ludwig-Maximilians-Universität zu München

Direktor: Prof. Dr. med. Reinhard Hohlfeld

**Identification and temporal stability of
conformational epitopes of autoantibodies
against Myelin Oligodendrocyte Glycoprotein
recognized by patients with different
inflammatory central nervous system diseases**

Dissertation

zum Erwerb des Doktorgrades der Humanbiologie (Dr. rer. biol. hum.) an
der Medizinischen Fakultät der Ludwig-Maximilians-Universität zu München



vorgelegt von

Marie Cathrin Mayer

aus Hamburg
2014

Mit Genehmigung der Medizinischen Fakultät der
Ludwig-Maximilians-Universität zu München

Berichterstatter: Prof. Dr. med. Edgar Meinl

Mitberichterstatter:

Prof. Dr. Ludger Klein

Priv. Doz. Dr. Ulrich Schüller

Prof. Dr. Dieter Edbauer

Dekan: Prof. Dr. med. Dr.h.c. Maximilian Reiser, FACR, FRCR

Tag der mündlichen Prüfung: 09.07.2014

Contents

1	Eidesstattliche Versicherung	5
2	Acknowledgments	6
3	Publications of the author	7
4	Abbreviations	9
I	Abstract/Zusammenfassung	10
5	Abstract	11
6	Zusammenfassung	14
II	Introduction	17
7	Inflammatory diseases of the central nervous system	18
8	Myelin Oligodendrocyte Glycoprotein (MOG)	19
9	Autoantibodies in encephalopathies and inflammatory CNS diseases	20
9.1	Autoantibodies contribute to CNS inflammation	20
9.2	Evidence for a pathogenic role of anti-MOG antibodies in humans	22
10	Treatment of inflammatory CNS diseases with therapeutics targeting B-cells and antibodies	22
11	Anti-MOG mAbs	24
12	Different detection methods for anti-MOG antibodies and contradictory results	24
12.1	Anti-MOG ELISA studies	24

12.2	Studies analyzing antibodies to native MOG	25
12.3	Stability of anti-MOG antibodies over time	26
13	Epitope mapping	27
13.1	Clinically relevant information gained from epitope mapping	27
13.2	Epitope spreading	27
III	Objectives	28
14	Objectives	29
IV	Material and Methods	30
15	Material	31
15.1	Chemicals and consumables	31
15.2	Antibodies	31
15.3	Patient samples	31
16	Methods	32
16.1	Determination of putative epitopes	32
16.2	Molecular cloning	33
16.2.1	PCR amplification of hMOG and mMOG from template vectors	33
16.2.2	Cloning of PCR products into pEGFP-N1 plasmid	35
16.2.3	Gel purification	35
16.2.4	Ligation	36
16.2.5	Transformation of <i>E. coli</i> DH5 α	36
16.2.6	Bacterial culture	37
16.2.7	Plasmid preparation	37
16.2.8	Mutagenesis	37

16.2.9	DNA sequencing	37
16.3	Cell culture of HeLa cells	38
16.4	Transfection of HeLa cells	38
16.5	Flow cytometric analysis of antibody binding	39
16.6	Competition assay	40
16.7	Preparation of cell lysates and deglycosylation by PNGase F	40
16.7.1	SDS PAGE	41
16.8	Western blot	41
16.9	IgG response to vaccines	41
V	Results	42
17	Cloning and expression of MOG constructs with a C-terminal, intracellular EGFP tag	43
18	Validation of transiently transfected MOG variants and reproducibility of binding ratios	45
19	Glycosylation of MOG-EGFP fusion proteins in HeLa cells	46
20	Recognition of MOG-epitopes analyzed with single and multiple amino acid mutants	47
20.1	Patients with anti-MOG IgG directed to one epitope	51
20.2	Patients with anti MOG IgG recognizing multiple epitopes	52
20.3	The triple mutant P42S/H103A/S104E	54
20.4	The N31D mutant	55
20.5	Higher reactivity to mutated variants of MOG	55
20.5.1	The S104E mutation could mimic phosphorylated MOG	56
20.6	Serial dilution of two sera showing differential recognition to MOG variants	56

21	Comparison of MOG epitope analysis with mutated variants versus competition with defined mAbs	59
22	MOG epitopes recognized by patients with different disease entities	59
23	Long term analysis of individual epitope patterns on MOG	61
24	Comparison of the dynamic of anti-MOG IgG with anti-measles virus and anti-rubella virus IgG	62
VI	Discussion	65
25	The polyclonal anti-MOG response is directed against amino acid loops . .	66
26	Species specific recognition	66
27	Expanding the model of hMOG	67
28	Pathogenicity of anti-MOG antibodies in humans	68
29	Assay comparison and evaluation	69
30	Relevance of MOG-glycosylation on recognition by human antibodies	70
31	Increased recognition of MOG mutant H103A/S104E	71
32	Temporal stability of epitope recognition	71
33	Stable IgG response upon vaccination in children rapidly losing anti-MOG IgG response	72
34	Therapeutic consequences	73
	Bibliography	74

1 Eidesstattliche Versicherung

Ich, Marie Cathrin Mayer, erkläre hiermit an Eides statt, dass ich die vorliegende Dissertation mit dem Thema “Identification and temporal stability of conformational epitopes of autoantibodies against Myelin Oligodendrocyte Glycoprotein recognized by patients with different inflammatory central nervous system diseases” selbständig verfasst, mich außer der angegebene(n) keinen weiteren Hilfsmittel bedient und alle Erkenntnisse, die aus dem Schrifttum ganz oder annähernd übernommen sind, als solche kenntlich gemacht und nach ihrer Herkunft unter Bezeichnung der Fundstelle einzeln nachgewiesen habe. Ich erkläre des Weiteren, dass die hier vorgelegte Dissertation nicht in gleicher oder in ähnlicher Form bei einer anderen Stelle zur Erlangung eines akademischen Grades eingereicht wurde.

Ort, Datum:

Unterschrift:

2 Acknowledgments

I am grateful to my supervisor Prof. Dr. Edgar Meinel for this exciting project. He was always available for my questions, generously shared his time and knowledge of MOG and always had faith in me and this project.

I would also like to thank my colleagues for the great time inside and outside of the lab and for the champagne. I was very lucky to be part of this team.

Heike Rübsamen, Robert Bittner and Petra Sperl did a great job providing an excellent infrastructure.

I would also like to thank our collaborators from other laboratories, especially Dr. Constanze Breithaupt and Prof. Dr. Markus Reindl who gave valuable input and who were inherent parts of this project, although I have never met them in person. This project would not have been possible without patient samples provided by Dr. Kevin Rostasy, Dr. Thomas Berger, Dr. Russell C. Dale, Dr. Fabienne Brilot, Dr. Tomas Olsson, Dr. Brenda Banwell and Dr. Amit Bar-Or.

Also, I would like to thank Prof. Dr. Hohlfeld, Prof. Dr. Wekerle and PD Dr. Dieter Jenne, who gave valuable intellectual input and asked important questions.

I am happy that Melania Spadaro has taken over the MOG project and I wish her perseverance, success and a lot of fun.

3 Publications of the author

Mayer MC, Breithaupt C, Reindl M, Schanda K, Rostásy K, Berger T, Dale RC, Brilot F, Olsson T, Jenne D, Pröbstel AK, Dornmair K, Wekerle H, Hohlfeld R, Banwell B, Bar-Or A, Meinl E

Identification of distinct epitopes on conformationally intact myelin oligodendrocyte glycoprotein recognized by human autoantibodies. *J Immunol.*, *in press*

Spadaro M*, Gerdes LA*, **Mayer MC***, Linn J, Zeller G, Krumbholz M, Hohlfeld R, Meinl E, Kümpfel T

Expanding clinical spectrum of myelin-oligodendrocyte glycoprotein antibody associated encephalomyelitis, *In preparation*

* These authors contributed equally.

Mayer MC, Hohlfeld R, Meinl E

Viability of autoantibody-targets: how to tackle pathogenetic heterogeneity as an obstacle for treatment of multiple sclerosis. *J Neurol Sci.* 2012 Aug 15;319(1-2):2-7

Mayer MC, Meinl E

Glycoproteins as targets of autoantibodies in CNS inflammation: MOG and more. *Ther Adv Neurol Disord.* 2012 May;5(3):147-59

Carafoli F, **Mayer MC**, Shiraishi K, Pecheva MA, Chan LY, Nan R, Leitinger B, Hohenester E

Structure of the discoidin domain receptor 1 extracellular region bound to an inhibitory Fab fragment reveals features important for signaling. *Structure.* 2012 Apr 4;20(4):688-97

Mayer MC

IgG directed against myelin oligodendrocyte glycoprotein (MOG)- Rapid disappearance in childhood acute disseminated encephalomyelitis (ADEM) and identification

of distinct epitopes.

Oral presentation given at the 10th B cell Forum of the DGfI Study Group “Biology of B Lymphocytes”, Kloster Banz, March 5-7, 2012

4 Abbreviations

Abbreviation	Meaning
aa	amino acid
AChR	actetylcholine receptor
ADEM	acute disseminated encephalomyelitis
AQP4	aquaporin-4
CNS	central nervous system
CSF	cerebrospinal fluid
CRION	chronic relapsing inflammatory optic neuritis
DNA	deoxyribonucleic acid
EGFP	enhanced green fluorescent protein
ELISA	enzyme linked immunosorbent assay
FACS	fluorescence-activated cell sorting
FCS	fetal calf serum
hMOG	human MOG
mAb	monoclonal antibody
MCF	mean channel fluorescence
mMOG	mouse MOG
MOG	myelin oligodendrocyte glycoprotein
mono ADS	patients experiencing only one acquired demyelinating event
MS	multiple sclerosis
NMO	neuromyelitis optice
ON	optic neuritis
PBS	phosphate buffered saline
PCR	polymerase chain reaction
TM	transverse myelitis

Part I

Abstract / Zusammenfassung

5 Abstract

Myelin Oligodendrocyte Glycoprotein (MOG) is one of the few proteins known to be localized on the outermost sheath of central nervous system (CNS) myelin. Due to this localization, MOG is accessible to antibodies. Anti-MOG antibodies are demyelinating and enhance clinical symptoms in a number of animal models of CNS inflammation.

Autoantibodies recognizing conformationally intact MOG are found in different inflammatory diseases of the CNS, but their antigenic epitopes had not been mapped. In this work, 9 variants of MOG with an intracellular enhanced green fluorescent protein (EGFP) tag were expressed on the cell surface of human HeLa cells and used to analyze sera from 111 patients (104 children, 7 adults), who had antibodies recognizing cell-bound human MOG. These patients had different diseases, namely acute disseminated encephalomyelitis (ADEM), one episode of transverse myelitis or optic neuritis, multiple sclerosis (MS), anti-aquaporin-4 (AQP4)-negative neuromyelitis optica (NMO), and chronic relapsing inflammatory optic neuritis (CRION).

The expression levels of the mutants were comparable and cells with a defined expression level (fluorescence intensity in the EGFP channel of 10^2 - 10^3) were gated. Each MOG-mutant was recognized by at least one MOG-specific mAb. This allowed the comparison of binding to the different mutants. In order to assess the reproducibility of the system, binding of the 111 sera to the mutants was analyzed up to three times in independent experiments, yielding a very good reproducibility of the binding percentage with an absolute SD of 7.8% in the case of low recognition of a mutant and a relative SD of 20% in the case of high recognition of a mutant.

The applied variants of MOG gave insight into epitope recognition of 98 patients. All epitopes identified in this work were located at loops connecting the β -strands of MOG. The immunodominant epitope of human anti-MOG antibodies was at the membrane-proximal CC'-loop containing aa42, which is not present in rodent MOG. This loop was recognized

by about half of all patients. Overall, seven epitope patterns were distinguished, including the one mainly recognized by mouse mAbs at the FG-loop around aa104. Evidence from mouse models of CNS inflammation shows that anti-MOG antibodies recognizing different epitopes can be demyelinating and thus pathogenic. This suggests that not only those antibodies recognizing the same epitope of MOG as the pathogenic mAbs (i.e. the FG-loop), but also the ones recognizing the CC'-loop are pathogenic in humans, as both epitopes allow for the recognition of cell-bound MOG.

In half of the patients, the anti-MOG response was directed to a single epitope. To analyze the effect of glycosylation on the recognition of MOG by human autoantibodies, a “non-glycosylation mutant” N31D was made. Digestion with PNGaseF and Western blot analysis confirmed that N31 was the only used N-glycosylation site of the MOG constructs in HeLa cells. Glycosylation of MOG was not needed for antibody binding, but 8% of the patients recognized deglycosylated MOG at least two-fold better.

The epitope specificity was not linked to certain disease entities. The individual epitope recognition patterns stayed constant in 11 analyzed patients over an observation period of up to 5 years without evidence for intramolecular epitope spreading. Some patients with acute syndromes had anti-MOG IgG at disease onset, but rapidly lost their anti-MOG IgG reactivity. These patients were able to generate a long-lasting IgG response to measles and rubella virus vaccine indicating that the loss of anti-MOG reactivity was not reflective of a lack of capacity for longstanding IgG responses.

Human anti-MOG antibodies are mainly of the IgG1 isotype, which can activate complement and antibody dependent cellular cytotoxicity. Upon binding to MOG in the CNS, human anti-MOG antibodies are hence expected to cause demyelination. Transfer experiments with purified human anti-MOG antibodies have not been performed yet. The fact that the majority of human anti-MOG antibodies did not recognize rodent MOG has implications for animal studies. Using the described assay will help to identify patient samples appropriate for these transfer experiments and finally lead to the formal proof of the

pathogenicity of human anti-MOG antibodies. This work also gives important information for future detection of potential mimotopes and the development of anti-MOG antibody detection assays and might pave the way to antigen-specific depletion.

6 Zusammenfassung

Das Myelin Oligodendrozyten Glykoprotein (MOG) ist eines der wenigen Proteine, von denen bekannt ist, dass sie sich auf der äußersten Schicht der Myelinscheide im zentralen Nervensystem (ZNS) befinden. Aufgrund dieser Lokalisation ist MOG für Antikörper erreichbar. Antikörper gegen MOG wirken in Tiermodellen demyelinisierend und verstärken dort die klinischen Symptome.

Antikörper gegen konformationelles MOG werden in unterschiedlichen entzündlichen Erkrankungen des ZNS gefunden, aber ihre antigenen Epitope wurden bisher nicht bestimmt. In dieser Arbeit wurden 9 MOG-Varianten mit intrazellulärer EGFP-Markierung auf der Zelloberfläche von HeLa-Zellen exprimiert und verwendet, um Seren von 111 Patienten (104 Kindern, 7 Erwachsenen) mit Antikörpern gegen zellgebundenes MOG zu untersuchen. Diese Patienten hatten unterschiedliche Krankheiten, namentlich akute disseminierte Enzephalomyelitis (ADEM), ein Ereignis einer transversen Myelitis oder Sehnerventzündung, Multiple Sklerose (MS), anti-Aquaporin-4 negative Neuromyelitis optica (NMO) und chronisch wiederkehrende Sehnerventzündung (CRION).

Der Expressionslevel der Mutanten war vergleichbar und es wurden Zellen mit einem definierten Expressionslevel (Fluoreszenzintensität im EGFP Kanal von 10^2 - 10^3) ausgewählt. Jede MOG Variante wurde von mindestens einem monoklonalen Antikörper erkannt. Somit konnte die Erkennung einzelner Mutanten untereinander verglichen werden. Um die Reproduzierbarkeit dieses Systems zu überprüfen, wurde die Bindung der 111 Seren zu den Mutanten bis zu dreimal in unabhängigen Experimenten gemessen. Die Ergebnisse waren sehr gut reproduzierbar, mit einer absoluten Standardabweichung von 7.8% bei geringer Erkennung einer Mutante und einer relativen Standardabweichung von 20% im Falle guter Erkennung einer Mutante.

Die eingesetzten MOG Varianten gaben Einblick in die Epitoperkennung von 98 Patienten. Alle in dieser Arbeit identifizierten Epitope befinden sich in den Schlaufen, die

die β -Stränge von MOG miteinander verbinden. Das immundominante Epitop humaner anti-MOG Antikörper lag an der membrannahen CC'-Schleufe, die die Aminosäure 42 enthält, welche in Maus-MOG nicht vorhanden ist. Diese Schleufe wurde von ungefähr der Hälfte der Patienten erkannt. Zusammen wurden sieben Epitop-Erkennungsmuster unterschieden, inklusive jenem um die FG-Schleufe mit Aminosäure 104, welches hauptsächlich von monoklonalen Maus Antikörpern erkannt wird.

In ungefähr der Hälfte der Patienten war die anti-MOG Antwort gegen ein einzelnes Epitop gerichtet. Um zu untersuchen, welche Rolle die Glykosylierung in der Erkennung von MOG durch humane Antikörper hat, wurde die "Nicht-Glykosylierungs-Mutante" N31D hergestellt. Verdau mit PNGase F und Western blot Analyse bestätigten, dass N31 die einzige verwendete N-Glykosylierungsstelle der MOG Konstrukte in HeLa Zellen war. Glykosylierung war für die Antikörperbindung nicht nötig, aber 8% der Patienten erkannten nicht glykosyliertes MOG mindestens doppelt so gut.

Es gab keine Verbindung zwischen Epitoperkennung und einer bestimmten Krankheit. Die individuellen Epitop-Erkennungsmuster blieben unverändert in 11 untersuchten Patienten über einen Beobachtungszeitraum von 5 Jahren, ohne dass es Hinweise auf intramolekulare Epitop-Ausweitungen gab. Einige Patienten mit akuten Erkrankungen hatten anti-MOG Antikörper in der akuten Phase ihrer Krankheit, aber verloren diese rasch. Diese Patienten konnten dennoch eine nachhaltige IgG Antwort zu einer Masern- und Rötelnviren Impfung bilden. Dies zeigt, dass der Verlust der anti-MOG Antwort nicht auf eine generelle Unfähigkeit, nachhaltige IgG Antworten zu bilden, zurückzuführen ist.

Menschliche anti-MOG Antikörper haben hauptsächlich den IgG1 Isotyp, der Komplement aktivieren und Antikörper-abhängige zelluläre Toxizität auslösen kann. Es wird erwartet, dass anti-MOG Antikörper, wenn sie MOG im ZNS binden, zu Demyelinisierung führen. Transferexperimente mit aufgereinigten MOG-Antikörpern wurden bisher nicht durchgeführt. Die Tatsache, dass die Mehrheit der menschlichen anti-MOG Antikörper Maus-MOG nicht erkannt haben, hat Konsequenzen für Tierstudien. Durch den Einsatz

des hier beschriebenen Verfahrens können Patientenproben identifiziert werden, die sich für diese Transferexperimente eignen und dies wird letztlich dazu führen, dass die Pathogenität von MOG-Antikörpern formal bewiesen wird. Diese Arbeit liefert darüber hinaus wichtige Informationen für die spätere Ermittlung potenzieller Mimotope und die Entwicklung von anti-MOG Antikörper-Assays und könnte den Weg zu einer Antigen-spezifischen Depletion ebnen.

Part II

Introduction

7 Inflammatory diseases of the central nervous system

There is a broad spectrum of inflammatory diseases of the central nervous system (CNS). Diseases investigated in this study include multiple sclerosis (MS), monophasic acquired demyelinating syndromes (mono ADS), acute disseminated encephalomyelitis (ADEM), Neuromyelitis optica (NMO) and Chronic relapsing inflammatory optic neuritis (CRION). An overview over these diseases is shown in figure 1. Most of the patients in this study are children, because anti-MOG antibodies are more common in children than in adults (see 12.2). MS is the most common, chronic inflammatory disease of the CNS, with a prevalence of 60-200/100.000 in Northern Europe and Northern America [Sospedra *et al.* 2005]. Pediatric MS is rare, accounting for only 3-5% of all MS cases. There are two major forms of MS: 85-90% of MS-patients show a relapsing-remitting course that usually changes to a secondary progressive form; 10-15% of the patients show a primary progressive form of MS. Mono ADS presentations include one episode of optic neuritis (ON), transverse myelitis (TM) or ADEM [Banwell *et al.* 2009], but in this work, ADEM will be treated separately. A proportion of 16-25% of children initially diagnosed with mono ADS, are finally diagnosed with MS before turning 18 [Banwell *et al.* 2009]. ADEM is an acute disorder of the CNS, which is most common in children younger than 10 years. ADEM is usually monophasic with a good prognosis. The majority of reported ADEM cases happened in the context of viral illness or vaccination [Tenembaum *et al.* 2002]. NMO is a very rare disease with a prevalence of only 0.5-4.4/100.000 [Jacob *et al.* 2013]. Importantly, NMO is a lot more common in Asia [Lennon *et al.* 2004]. NMO is characterized by recurrent optic neuritis and longitudinally extended transverse myelitis spanning more than three vertebral segments. The majority of NMO patients has antibodies against AQP4 [Weinshenker *et al.* 2006]. CRION is a not well understood condition characterized by recurrent painful inflammation of the optic nerves causing subacute visual loss [Kidd *et al.* 2003]. CRION patients respond well to corticosteroid treatment and usually do not have white matter lesions.

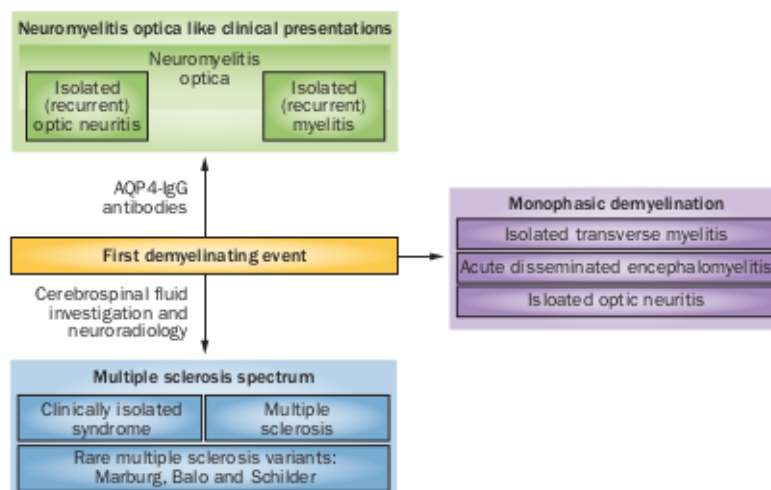


Figure 1: Acquired CNS inflammatory demyelinating diseases. This figure was taken from [Reindl *et al.* 2013].

8 Myelin Oligodendrocyte Glycoprotein (MOG)

MOG is a small (218 amino acids) and quantitatively minor component of CNS myelin (less than 0.05% of all CNS myelin proteins). It is found on the outermost surface of myelin [Brunner *et al.* 1989]. Other more abundant myelin components, such as myelin basic protein, are not found on the surface of CNS myelin and are hence inaccessible for antibodies. Human MOG has not yet been crystallized, but crystal structures of rat MOG together with the Fab fragment of the mAb 8-18C5 [Breithaupt *et al.* 2003] and mouse MOG [Clements *et al.* 2003] have been published. MOG features an IgV-like fold (see figure 2) with a single glycosylation site N31 [Gardinier *et al.* 1993]. The exact function of MOG is not known, but its structure and localization suggest a role as an adhesion molecule, possibly gluing CNS myelin fibers together [Clements *et al.* 2003]. MOG itself is also able to bind the complement component C1q and might therefore regulate the classical complement pathway [Johns *et al.* 1997]. MOG might also function as a host cell receptor for the rubella virus [Cong *et al.* 2011]. A MOG knockout mouse, however, showed no obvious phenotype [Delarasse *et al.* 2003].

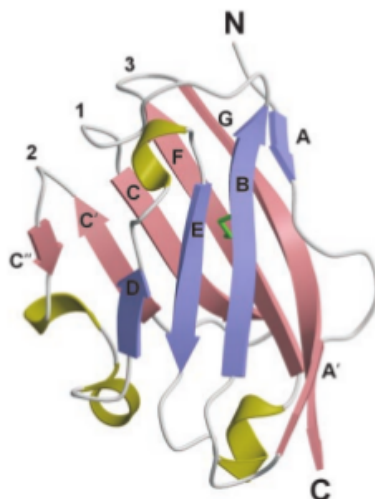


Figure 2: IgV like fold of mMOG. This figure was taken from [Clements *et al.* 2003].

9 Autoantibodies in encephalopathies and inflammatory CNS diseases

9.1 Autoantibodies contribute to CNS inflammation

Autoantibodies are important players in a number of inflammatory CNS diseases [Vincent *et al.* 2011, Lancaster *et al.* 2012, Iorio *et al.* 2012, Krumbholz *et al.* 2012, Srivastava *et al.* 2012, Quintana *et al.* 2008]. Plasma exchange is effective in removing antibodies from the circulation and is a useful therapy option for a subset of MS [Keegan *et al.* 2005, Magana *et al.* 2011] and NMO patients [Kim *et al.* 2013]. The success of this therapy proves the pathogenic potential of autoantibodies. Transfer studies, in which human anti-AQP4 antibodies were injected into animals, have proven the pathogenic potential of these anti-AQP4 antibodies in NMO [Bennett *et al.* 2009, Bradl *et al.* 2009, Saadoun *et al.* 2010, Kinoshita *et al.* 2009]. MOG is one of the few proteins known to be localized on the outermost surface of CNS myelin [Brunner *et al.* 1989] (see figure 3). MOG is hence accessible for pathogenic autoantibodies, as reviewed in [Mayer *et al.* 2012].

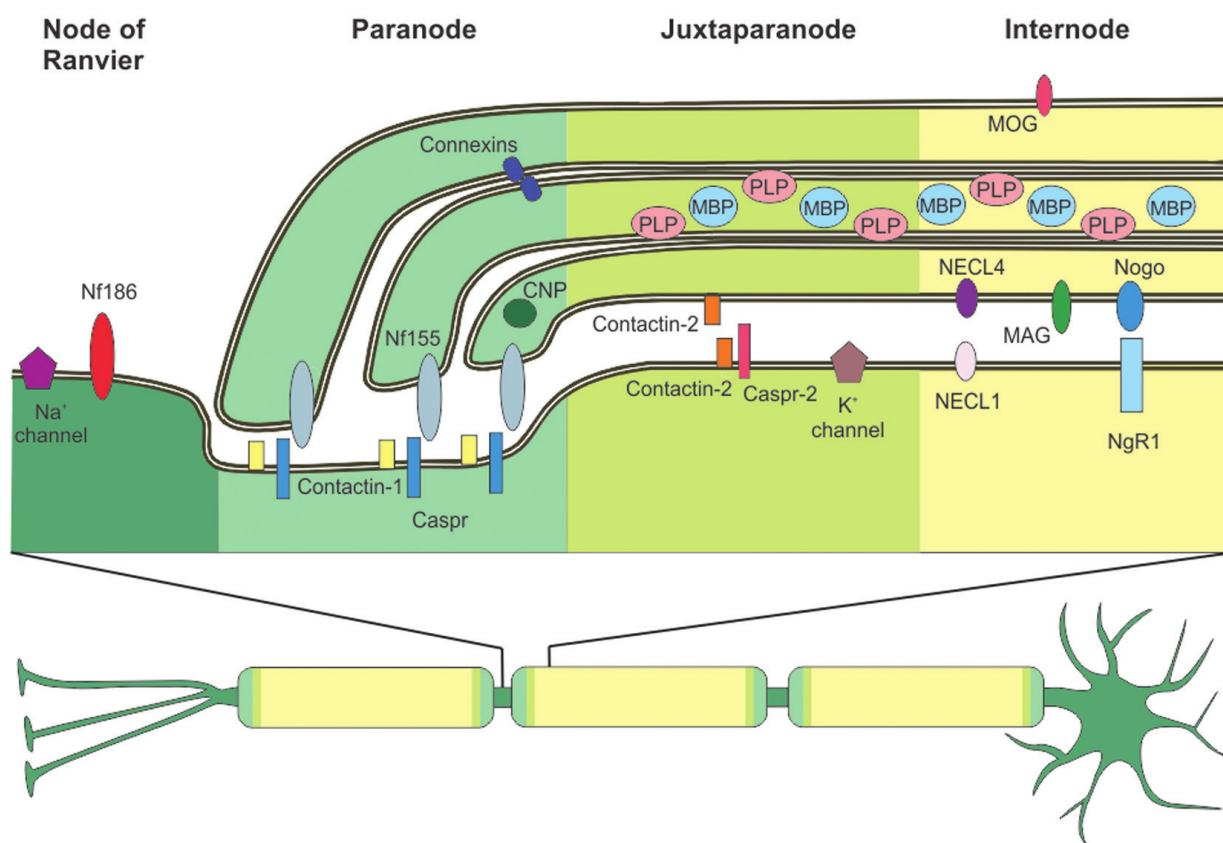


Figure 3: The position of MOG in CNS myelin. (This figure was taken from [Mayer *et al.* 2012], it was created by the author of this thesis.) A neuron with a myelinated axon is depicted. Myelin enwraps the axon at intervals called internodes omitting small openings termed nodes of Ranvier. The zones next to the nodes of Ranvier are the paranode and the juxtaparanode. All four zones have a characteristic protein composition, as marked in the upper part of the picture. Typical myelin proteins are found at the internode: Proteolipid protein (PLP) and Myelin basic protein (MBP) are the major myelin proteins. MOG is a minor component of myelin and one of the few proteins known to be localized on the surface of the myelin sheath.

9.2 Evidence for a pathogenic role of anti-MOG antibodies in humans

Anti-MOG antibodies are pathogenic in rodents [Linington *et al.* 1988, Schluesener *et al.* 1987] and primates [Genain *et al.* 1995]. A pathogenic role of anti-MOG antibodies in CNS inflammation is supported by several observations. First, anti-MOG antibodies found in subgroups of inflammatory diseases recognize cell-bound MOG (see below). Second, the demyelinating activity of anti-MOG antibodies in animal models correlates with their ability to fix complement [Piddlesden *et al.* 1993]. Human anti-MOG antibodies are mostly of the complement activating isotype IgG1 [Proebstel *et al.* 2011, McLaughlin *et al.* 2009, Mader *et al.* 2011]. Antibody-dependent cellular cytotoxicity activity of human anti-MOG antibodies has also been observed *in vitro* and is likely to contribute to the pathogenicity of these antibodies [Brilot *et al.* 2009]. Third, anti-MOG antibodies require a breached blood–brain barrier to enter the CNS; they are not pathogenic in the absence of CNS inflammation [Litzenburger *et al.* 1998]. In a T-cell-mediated encephalitis, the blood-brain barrier is breached, which is demonstrated by gadolinium-enhancing lesions in the majority of pediatric MS and ADEM patients [Poser *et al.* 2007, Waubant *et al.* 2009].

10 Treatment of inflammatory CNS diseases with therapeutics targeting B-cells and antibodies

A detailed overview about the role of B-cells in the treatment of MS is given in [Krumbholz *et al.* 2012]. Figure 4 gives an overview over the possible roles of B-cells in autoimmune processes. NMO patients benefit from an anti-CD20 treatment with the monoclonal antibody (mAb) rituximab [Pellkofer *et al.* 2011], that depletes CD20⁺ B-cell lineage cells in blood, CSF and tissue [Hauser *et al.* 2008]. In a phase II clinical trial, rituximab

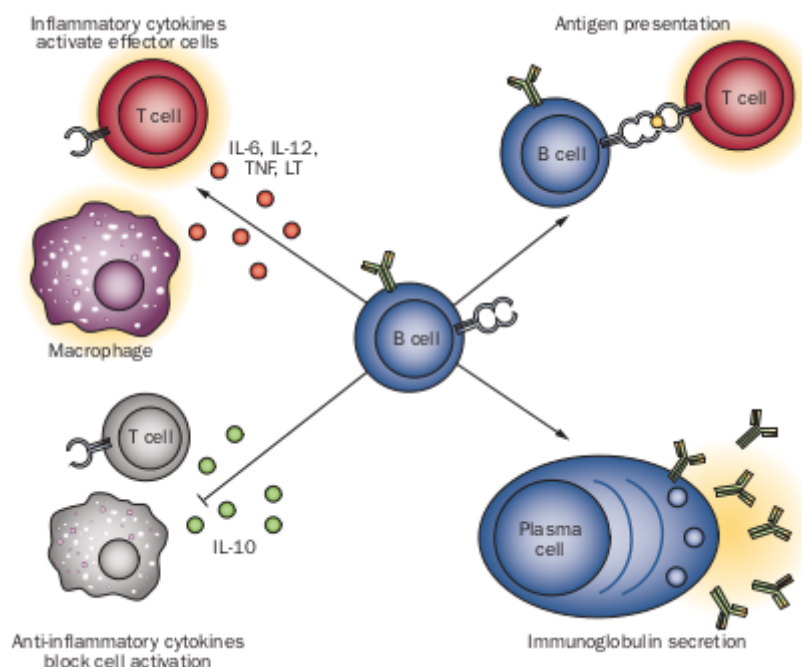


Figure 4: Possible roles of B-cells in the pathogenesis of inflammatory CNS diseases. This figure was taken from [Krumbholz *et al.* 2012].

also showed great success in treating relapsing-remitting MS patients [Hauser *et al.* 2008]. Another anti-CD20 mAb ocrelizumab was also very effective in a phase II clinical trial in reducing the number of gadolinium-enhancing lesions, but showed serious side effects [Kappos *et al.* 2011]. The effect of these therapeutics on autoantibody levels is unclear, rituximab reduced anti-AQP4 levels in some, but not all NMO patients [Pellkofer *et al.* 2011]. The anti α 4-integrin mAb natalizumab is an approved second-line therapeutic for relapsing-remitting MS. Natalizumab prevents α 4-integrin-mediated adhesion and transmigration of B cells, T cells, and monocytes from the blood into the CNS [Ransohoff *et al.* 2012]. The sphingosine-1-phosphate receptor modulator FTY720 is also approved as a second-line treatment in relapsing-remitting MS. It reduces the immune-cell exit from lymphatic tissue and also has local effects in the CNS [Aktas *et al.* 2010]. Acute inflammatory diseases like ADEM and ON, as well as MS relapses are treated with steroids. Steroids have a number of effects on the immune system, including apoptosis of B-cells [Andri eau *et al.* 1998].

11 Anti-MOG mAbs

A number of mouse mAbs against MOG are available. The first and most prominent one is 8-18C5 [Linnington *et al.* 1984]. This mAb was raised against rat cerebellar glycoproteins. It cross-reacts with murine and human MOG. This mAb is of the IgG1 isotype. An additional 13 anti-MOG mAbs were raised against bovine lentil lectin-binding proteins (Y1, Y2, Y4, Y6, Y7, Y8, Y9, Y10 and Y11) or partially purified bovine MOG (Z2, Z4, Z8 and Z12) [Piddlesden *et al.* 1993]. All of these mAbs have the isotype IgG1, with the exceptions of Z2, Z4, and Z12, which are IgG2a. In this study, the two mAbs 8-18C5 and Y11 were used, as they have been shown to recognize different epitopes [Brehm *et al.* 1999, Breithaupt *et al.* 2008]. Both mAbs are pathogenic in experimental autoimmune encephalitis [Piddlesden *et al.* 1993].

12 Different detection methods for anti-MOG antibodies and contradictory results

12.1 Anti-MOG ELISA studies

Numerous studies have analyzed anti-MOG antibodies in different patient groups [Mayer *et al.* 2012]. Early studies of anti-MOG antibodies in MS patients used an enzyme-linked immunosorbent assay (ELISA) to determine the anti-MOG antibody titer in patients' sera and cerebrospinal fluid (CSF) [Xiao *et al.* 1991]. Using this technique, anti-MOG antibodies were detected in the CSF of a subset of MS patients, but also in the control groups. Later studies analyzed the recognition of MOG peptides: anti-MOG antibodies were isolated by affinity chromatography to MOG coupled agarose and the binding of these antibodies to synthetic MOG peptides was assessed in an ELISA [Haase *et al.* 2001]. Antibodies from both patients and controls recognized several pep-

tides and no specific MS-associated binding pattern was found. Only one out of these 17 MS samples and none of the nine healthy controls also recognized cell-bound MOG in a flow-cytometry assay [Haase *et al.* 2001]. This implies that antibodies to MOG peptides are found both in patients and in healthy controls, but only a subset of patients has antibodies recognizing cell-bound MOG. Evidence from animal models shows that recognition of cell-bound MOG is a prerequisite for the pathogenicity of anti-MOG antibodies [Brehm *et al.* 1999, Bîçœdingen *et al.* 2004].

12.2 Studies analyzing antibodies to native MOG

A major breakthrough in the understanding of antibodies to MOG came with a study analyzing ADEM patients along with adult MS patients [O'Connor *et al.* 2007]. This study used both cell-bound MOG and a tetramer-based assay radioimmunoassay. It showed that a proportion of ADEM patients have high anti-MOG antibody levels, while these antibodies are rare in adult MS and only present at low levels [O'Connor *et al.* 2007]. Recent studies used cell-bound MOG assays to detect and quantify anti-MOG antibodies by FACS or immunocytochemistry [Brilot *et al.* 2009, Di Pauli *et al.* 2011, Lalive *et al.* 2011, McLaughlin *et al.* 2009, Proebstel *et al.* 2011, Kitley *et al.* 2012, Mader *et al.* 2011, Rostasy *et al.* 2013]. Using cell-bound MOG assays, anti-MOG antibodies were found in a proportion of children with ADEM [Proebstel *et al.* 2011, Mader *et al.* 2011, McLaughlin *et al.* 2009, Brilot *et al.* 2009], pediatric MS [Proebstel *et al.* 2011, McLaughlin *et al.* 2009, Lalive *et al.* 2011, Di Pauli *et al.* 2011], children with optic neuritis (ON) and children with recurrent ON [Rostasy *et al.* 2012], in a subgroup of anti-AQP4 negative pediatric and adult NMO patients and patients at high risk of developing NMO [Kitley *et al.* 2012, Mader *et al.* 2011, Rostasy *et al.* 2013].

12.3 Stability of anti-MOG antibodies over time

Two studies have analyzed the stability of anti-MOG antibodies over time [Di Pauli *et al.* 2011, Proebstel *et al.* 2011]. A correlation was seen between a decline in antibody titers and full recovery in ADEM patients [Di Pauli *et al.* 2011]. All 16 ADEM patients analyzed in a 5-year follow up study, had rapidly declining anti-MOG antibodies, while anti-MOG antibodies detected in the same study in pediatric MS patients persisted in six of eight patients with fluctuations and were even shown to increase [Proebstel *et al.* 2011], see also figure 5.

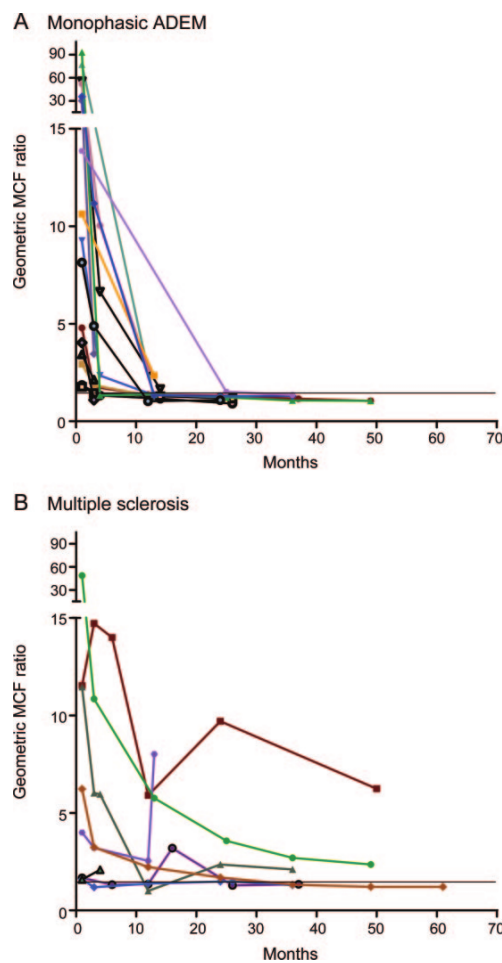


Figure 5: Anti_MOG antibodies decline rapidly in ADEM patients and persist in most pediatric MS patients. This figure was taken from [Proebstel *et al.* 2011].

13 Epitope mapping

13.1 Clinically relevant information gained from epitope mapping

Mapping of antibody epitopes allows precise insight into molecular effects exerted by antibodies and gave important insights into a variety of different disorders. In the case of anti-erythropoietin autoantibodies in HIV-patients, the immunodominant antibody-epitopes correspond to the part of erythropoietin that is recognized by the erythropoietin receptor, this might contribute to a dysregulation of erythropoietin and contribute to HIV-related anemia [Tsiakalos *et al.* 2011]. In some cases, epitope mapping allowed a differentiation between patient groups: patients with inflammatory bowel disease and coronary heart disease have antibodies against heat shock proteins 60 and 65. These antibodies are also found in healthy controls, but the epitopes differed between the three investigated groups [Fust *et al.* 2012].

13.2 Epitope spreading

Autoantibody epitope spreading has been described in the context of a number of autoimmune diseases. In an animal model of myasthenia gravis, peptides of the acetylcholine receptor (AChR) were injected into rabbits, which subsequently produced antibodies not only against these peptides, but also against other parts of the protein [Vincent *et al.* 1994]. Antimitochondrial antibodies in Primary biliary cirrhosis patients show intra- and intermolecular epitope spreading [Mori *et al.* 2012]. Intermolecular epitope spreading of anti-citrullinated protein antibodies is a predictor of progression to rheumatoid arthritis [Sokolove *et al.* 2012].

Part III

Objectives

14 Objectives

Autoantibodies to MOG are found in subgroups of different disease entities. Before this project, the epitopes of these antibodies were not known. The objectives of this work were 1. Definition of epitopes recognized by human autoantibodies on conformationally intact MOG expressed on the cell surface. 2. Assessment of the distribution of recognized epitopes in a single patient- is the autoantibody response in a single patient directed against an immunodominant epitope or is it broadly distributed? 3. Assessment of a possible linkage between disease entity and epitope recognition. 4. Analysis of the stability of epitope patterns in individual patients over years. 5. Evaluation of the general ability of producing a persisting IgG response in patients with a rapidly declining anti-MOG IgG response.

Part IV

Material and Methods

15 Material

15.1 Chemicals and consumables

Chemicals were purchased from Sigma-Aldrich (Munich, Germany) or Merck (Darmstadt, Germany), unless otherwise specified below. Consumables like pipette tips centrifuge tubes were purchased from either Eppendorf (Hamburg, Germany) or BD Falcon (Heidelberg, Germany). Cell-culture material was obtained from Corning (Wiesbaden, Germany) and Nunc (Langenselbold, Germany).

15.2 Antibodies

The antibodies for the FACS and Western Blot experiments are summarized in table 1.

Target specificity	source	Company	Catalogue no.	Tag
Anti-human IgG, Fc γ	goat	Jackson Immuno Research	109-066-098	Biotin
Anti-mouse IgG, Fc γ	goaat	Jackson Immuno Research	115-066-003	Biotin
Streptavidin		Jackson Immuno Research	016-190-084	Dy light 649
Anti-GFP	rabbit	Research Diagnostics	n/a	-
Anti-rabbit IgG	goat	Dianova	111-035-006	HRP

Table 1: Antibodies used in this study

15.3 Patient samples

This study included sera of 111 patients with different inflammatory CNS diseases and antibodies to cell-bound MOG: mono ADS, ADEM, MS, NMO, CRION and other relapsing ADS cases (table 2). Of these, 7 patients were adults (18 or older). 54 of these patients had been recognized as anti-MOG positive in previous studies, 57 additional patients were newly identified as anti-MOG positive using our cell-bound assay with transiently transfected cells from a cohort of 188 pediatric patients with inflammatory CNS diseases. The proportion of sera identified as positive in this cohort was: ADEM 41%, MS 5%, mono ADS 29%, other

relapsing cases 80%, CRION 100%. This study was approved by local ethical committees, and informed consent was obtained from all patients, parents, or legal guardians.

Disease	Number of patients with antibodies to hMOG (adults)	Number females	Age mean in years (range)
Mono ADS other than ADEM	45 (2)	25	11.0 (1.5-51.8)
ADEM	40 (1)	19	7.0 (1.4-47.1)
MS	10 (1)	7	11.3 (3.4-34)
NMO like	2 (1)	1	34.7 (13.5-55.9)
CRION	10 (2)	6	15.3 (7.4-32)
Other relapsing ADS	4	1	7.9 (3.2-15.7)

Table 2: Patient data. Other relapsing ADS cases: three patients had one ADEM attack plus one non- ADEM attack, and one patient had a monolesional transverse myelitis.

16 Methods

16.1 Determination of putative epitopes

The tip of the FG-loop of MOG is recognized by the mAb 8-18C5 . Hence the two amino acids H103 and S104 were mutated to obtain H103A/S104E. The single amino acid mutant S104E was also mutated, since this mutant already reduced binding of rMOG to mAb 8-18C5 by >40% . MOG is glycosylated at N31. In order to analyze the contribution of the glycosylation for antibody recognition, N31D was chosen as an unglycosylated MOG-mutant. Because recognition of mMOG was dramatically reduced in the majority of patients, three mutants of hMOG with the corresponding murine amino acids were chosen (see figure 6). Dr. Constanze Breithaupt helped with the analysis of the differences between human and murine amino acids. The chosen mutations were very surface exposed in the structure of mMOG and non-conservatively substituted in the sequence of hMOG: P42S, R9G/H10Y and R86Q.

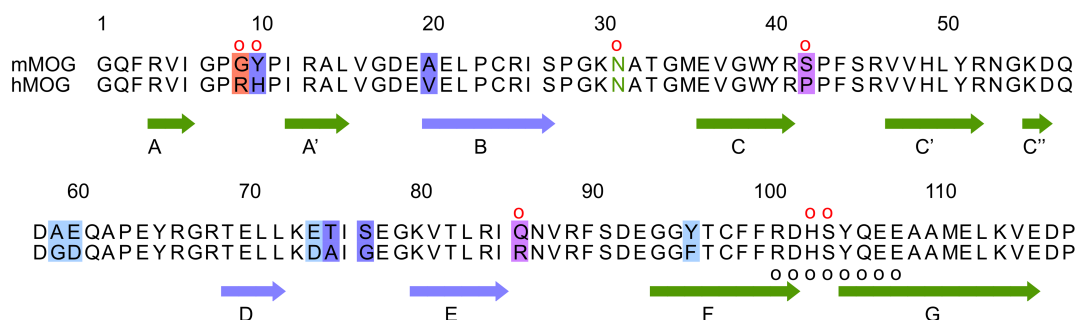


Figure 6: Protein sequence alignment of the Ig-V like domain of human MOG (hMOG) and of murine MOG (mMOG). This figure was taken from [Mayer *et al.* 2013] and was prepared by Dr. Constanze Breithaupt. The amino acid residues are highlighted in color reflecting the sequence conservation of hMOG and mMOG along the spectrum (white indicates identical residues; blue, purple and red indicate least conservative substitutions). The glycosylation site Asn31 is shown in green. Below the alignment, the secondary structure elements of mMOG are shown. The arrows labeled A to G represent the strands of the β -sheet. The green strands represent the front side and the blue strands the back side of the protein. The FG-loop and neighboring residues representing the center of the epitope on rat MOG (rMOG) recognized by mAb 8-18C5 are marked by black circles. Residues which have been mutated in this study are marked with a red circle.

16.2 Molecular cloning

16.2.1 PCR amplification of hMOG and mMOG from template vectors

Full length hMOG and mMOG were subcloned into the pEGFP-N1 plasmid (CLONTECH Laboratories, Inc., Mountain View, USA) in order to make MOG-EGFP fusion proteins, with the EGFP being at the C-terminus of MOG (see figure 7).

The primers were manufactured by Metabion (Martinsried, Germany) and are listed in table 3. The templates used were hMOG in RSV5'neo and mMOG in pLXSN. To amplify the DNA inserts from the templates, a PCR reaction was performed using the reagents shown in table 4. All reagents were mixed and a PCR was performed using the program shown in table 5. The PCR product was purified using the Qiagen PCR purification kit (Qiagen, Hilden, Germany). The DNA was eluted in 30 μ L EB buffer (Qiagen).

Name	Description	Sequence
CM3	hMOG forward, with XhoI restriction site	5'-GGC TGC AGC TCG AGA TGG C-3'
CM4	hMOG reverse, with <i>EcoRI</i> restriction site	5'-TGT CTG GGA ATT CGG AAG GGA TTT CG-3'
CM5	mMOG forward, with XhoI restriction site	5'-CGG TAA CCC TCG AGA TGG CCT GTT TGT-3'
CM6	mMOG reverse, with <i>EcoRI</i> restriction site	5'-CAC AAC CAG AAT TCG AAA GGG GTT TCT-3'

Table 3: Primers used for amplification of hMOG and mMOG

Reagent	Volume used	Stock concentration of reagent
DNA template	5 μ L	10 pg/ μ L
dNTPs	1 μ L	2 mM
Taq polymerase	0.5 μ L	5 U/ μ L
Forward primer	2 μ L	10 μ M
Reverse primer	2 μ L	10 μ M
Taq buffer	5 μ L	10x
Water	24.5 μ L	

Table 4: Reagents for the PCR reaction

Stage	Temperature	Time	
Denaturation	94°C	3 minutes	
Denaturation	94°C	30 seconds	30 repeats
Annealing	56°C	30 seconds	
Extension	72°C	1 minute	
Extension	72°C	10 minutes	
Cooling	4°C		

Table 5: PCR program

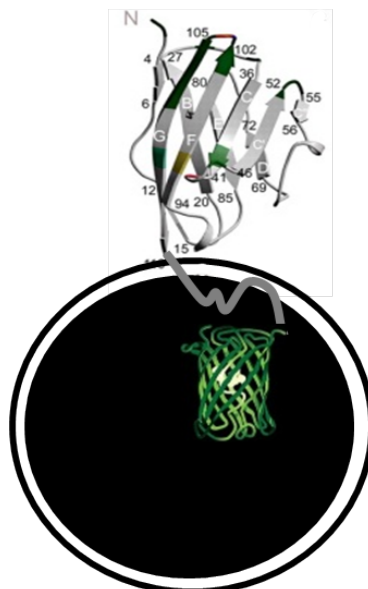


Figure 7: Model of a MOG-EGFP fusion protein in a cell. The MOG-model was taken from [Breithaupt *et al.* 2008]. The membrane topology was modeled according to [Della Gaspera *et al.* 1998]. This demonstrates that the EGFP-tag is intracellular at the C-terminus of MOG.

16.2.2 Cloning of PCR products into pEGFP-N1 plasmid

The purified PCR products and the pEGFP-N1 plasmid (figure 8) were digested with the restriction enzymes XhoI and *EcoRI*. For this reaction, 1 μg vector or the entire purified PCR product were added to the digestion mix containing 1 μL XhoI, 1 μL *EcoRI*, 0.1 μg bovine serum albumine and 1x reaction buffer 4 (New England Biolabs, Ipswich, USA). The digestion was performed at 37°C for 1h. The digested DNA was then gel purified.

16.2.3 Gel purification

In order to purify DNA of a desired size from a gel containing multiple DNA fragments, the gel was exposed to low intensity (312 nm) UV light and the desired fragment was cut out using a scalpel. The DNA was then purified from the gel using the QIAquick Gel Extraction Kit (Qiagen), according to the manufacturer's protocol.

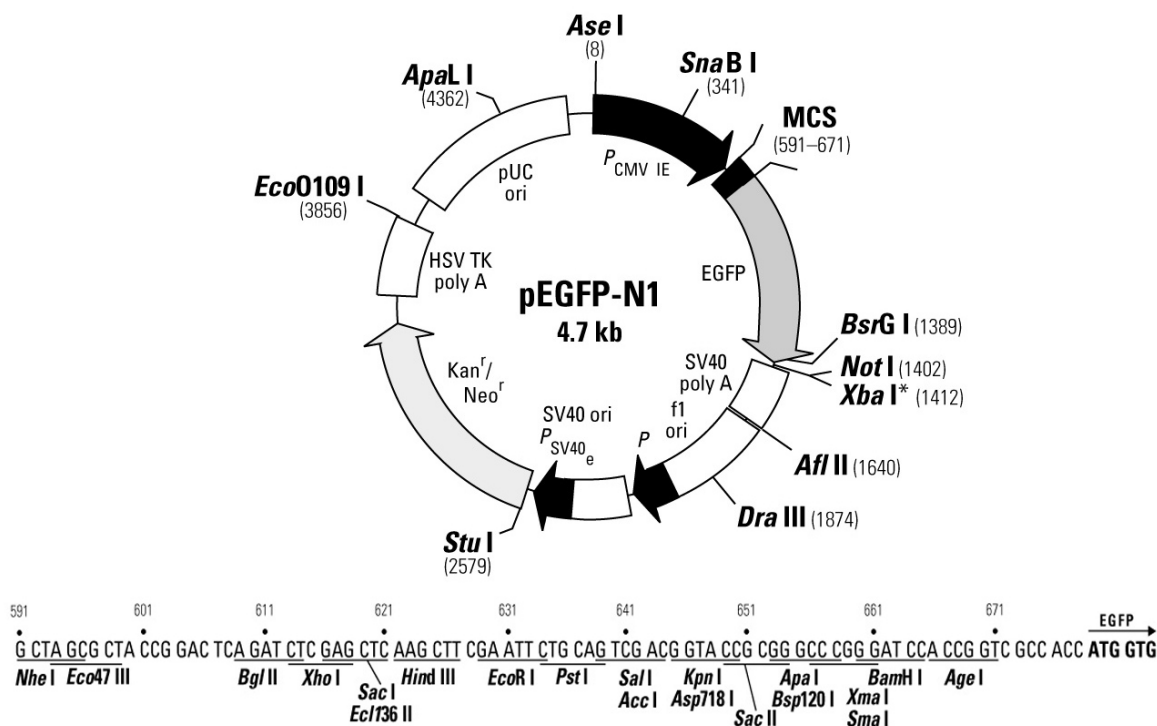


Figure 8: Vector pEGFP-N1 (picture taken from <http://www.human.cornell.edu>)

16.2.4 Ligation

Digested and purified pEGFP-N1 and PCR products were ligated using T4 DNA ligase. To this end, 50 ng of the digested vector and insert in different molar ratios (usually 1:5) were added to a ligation mix. The ligation mix consisted of 1 μ L T4 DNA ligase (Invitrogen) and 1x T4 DNA ligase buffer (Invitrogen). The ligation reaction was performed at 16°C for 1h. The reaction was stopped by a heat inactivation of the ligase at 65°C for 15 minutes.

16.2.5 Transformation of *E. coli* DH5 α

A 10 μ L aliquot of the ligated DNA was added to a 50 μ L aliquot of competent *E. coli* DH5 α cells. This mixture was incubated on ice for 20 minutes. A heatshock reaction was performed for 90 seconds at 42°C. The reaction mix was kept on ice for 4 minutes and 450 μ L LB medium were added. The transformed cells were incubated in a shaker at 37°C for

45 minutes to allow for regeneration. The complete reaction was plated onto LB plates containing 30 mg/mL Kanamycin. The plates were incubated overnight at 37°C.

16.2.6 Bacterial culture

A single transformed *E. coli* DH5 α cell was picked and added to LB medium containing 30 mg/mL kanamycin. Bacteria were grown while shaking at 37°C overnight. For minipreps, 2 mL were inoculated and for maxipreps 100 mL.

16.2.7 Plasmid preparation

Plasmids were prepared from overnight cultures using the Qiaspin Plasmid Miniprep kit (Qiagen) or the Qiaspin Plasmid Maxiprep Kit (Qiagen). To confirm the correct size of the purified DNA and the presence of an insert, a small amount of DNA, usually 200 ng, was digested with restriction enzymes and analyzed on an agarose gel.

16.2.8 Mutagenesis

Using the “QuikChange Site-Directed Mutagenesis” kit (Stratagene, Santa Clara, USA), point mutations were introduced into hMOG using the primers shown in table 6 and the corresponding reverse complement primers. In the case of the P42S/H103A/S104E mutant, the P42S mutation was introduced into the H103A/S104E mutant.

16.2.9 DNA sequencing

The DNA was sequenced in order to exclude PCR-generated errors at the MPI of Biochemistry and the LMU Biocenter (both in Martinsried, Germany).

Mutation	Sequence forward primer
S104E	5'-CCT GCT TCT TCC GAG ATC ATG AAT ACC AAG AGG AGG C-3'
H103A/S104E	5'-CCT GCT TCT TCC GAG ATG CTG AAT ACC AAG AGG AGG CAG-3'
N31D	5'-CAT ATC TCC TGG GAA GGA CGC TAC AGG CAT GGA GG-3'
R9G/H10Y	5'-CAG AGT GAT AGG ACC AGG ATA CCC TAT CCG GGC TCT GG-3'
R86Q	5'-GGT GAC TCT CAG GAT CCA GAA TGT AAG GTT CTC AGA TG-3'
P42S and P42S/H103A/S104E	5'-GTG GGG TGG TAC CGC TCC CCC TTC TCT AG-3'
P42S (Innsbruck)	5'-GTG GGG TGG TAC AGA TCT CCC TTC TCT AGG-3'

Table 6: Primers used for the QuikChange protocol

16.3 Cell culture of HeLa cells

HeLa cells were cultured in Dulbecco's Modified Eagle's Medium (DMEM) (Invitrogen) containing 10% fetal calf serum (FCS) (Gibco) and 1% Penicillin/Streptomycin solution (Gibco). The cells were cultured in T75 tissue culture flasks (BD Biosciences) at 37°C and 10% CO₂ and split 1:2 every 2-3 days. To this end, cells were washed once with phosphate-buffered saline (PBS) (Invitrogen) and trypsinized for about 5 minutes at 37°C with 2 mL trypsin-EDTA (Invitrogen). Trypsinization was stopped by the addition of 10mL complete medium.

16.4 Transfection of HeLa cells

HeLa cells were transiently transfected with using Metafectene transfection reagent (Biontex, Martinsried, Germany). On the day of transfection, cells were usually 90% confluent. The cells were trypsinized and suspended in 20 mL fresh complete medium. Subsequently, the cells were pelleted at 1200 rpm and resuspended in 40 mL complete medium. Per 60mmØ dish, 4.5mL cell suspension were plated. The cells were kept at 37°C and 10%

CO₂ for no longer than 30 minutes. During this time, the transfection mix was prepared for every well. In one tube, 7.5 µg DNA were added to 250 µL PBS. In a second tube, 60 µL Metafectene was added to 250 µL PBS. The content of the first tube was then added to the second tube and this mixture was incubated at room temperature for 15 minutes. After this incubation time, the transfection mix was added to cell dishes. The cells were incubated at 37°C and 10% CO₂ overnight.

16.5 Flow cytometric analysis of antibody binding

HeLa cells transiently transfected with EGFP only, hMOG-EGFP, mMOG-EGFP and mutants of hMOG-EGFP were assessed for their recognition by human sera. To this end, transiently transfected HeLa cells were washed with PBS and trypsinized. After suspension in complete medium, the cells were pelleted and resuspended in FACS buffer (1% fetal calf serum in phosphate-buffered saline). In a 96-well plate, 100,000 cells were incubated with a 1:50 serum dilution for 45 minutes at 4°C and washed 3 times in FACS buffer. The cells were then incubated with a 1:500 dilution of a biotin-SP conjugated goat anti-human IgG (Jackson ImmunoResearch) for 30 minutes at 4°C, washed 3 times and incubated with streptavidin-Dy light 649 (Jackson ImmunoResearch) at a dilution of 1:3000). Finally, the cells were washed 3 times and suspended in a 1:500 dilution of propidium iodide in PBS. The stained cells were analyzed using a BD FACSCalibur flow cytometer. Dead cells were excluded by positive propidium iodide staining. For binding analysis, the cells showing a 100-fold higher FL-1 fluorescence intensity as the untransfected cells were gated (expression level FL-1 10²-10³) and the mean channel fluorescence (MCF) in the FL-4 channel was obtained for these cells. Cells transfected with the mutants, hMOG and with EGFP only were always measured together in the same experiment in order to determine the binding percentage as $\%binding = \frac{MCF(mutant) - MCF(EGFP-only)}{MCF(hMOG) - MCF(EGFP-only)}$. In addition, two sera (adult ADEM patient 18078 and TM patient AEB-123) were serially diluted in FACS

buffer up to a dilution of 1/12800 and the dilutions were used to perform the FACS assay as described above, in order to show that the binding patterns stay constant at higher dilutions.

16.6 Competition assay

For competition of the human antibodies, the anti-MOG mAbs 8-18C5 and Y11 were added to the 1:50 serum dilution at 240ng/well and the transfectants were incubated with the mixture of serum and mAbs and developed with a 1:500 dilution of biotin-SP conjugated goat anti-human IgG (Jackson ImmunoResearch) and streptavidin-Dy light 649 1:3000 (Jackson ImmunoResearch) as described above. This anti-human secondary Ab did not cross-react with the murine mAbs (data not shown).

16.7 Preparation of cell lysates and deglycosylation by PNGase F

In order to analyze the glycosylation of the different MOG-EGFP constructs, HeLa cells were transiently transfected with MOG-EGFP constructs, as described above. The cells from a 12-well plate well were suspended in 1 mL PBS then pelleted at 13,000 rpm for 2 minutes in a bench top centrifuge. The pellets were washed in 1 mL cold PBS and pelleted again. The cells were then lysed at 4°C for 1h in 80 µL RIPA buffer (150 mM NaCl, 1% NP-40, 0.5% sodium deoxycholate, 50 mM Tris pH8, 0.1% SDS) containing complete protease inhibitor cocktail (Roche Applied Science, Penzberg, Germany). The lysate was then pelleted at 13,000 rpm for 10 minutes and the supernatant was analyzed. For deglycosylation, the supernatant was digested with PNGaseF (New England Biolabs) in Glycoprotein Denaturing Buffer (New England Biolabs), G7 Reaction Buffer (New England Biolabs) and 1% NP40 (New England Biolabs) at 37°C overnight.

16.7.1 SDS PAGE

The total protein concentration of the lysates was determined using a BCA protein assay reagent kit (Pierce, Rockford, USA) according to the instructions of the manufacturer. 6 μ g protein (digested or undigested) was loaded onto an precast 4-12% Bis-Tris gels (Invitrogen) and separated by gel electrophoresis at 200V for 90 minutes.

16.8 Western blot

The proteins were electro-blotted onto a nitrocellulose membrane at 100mA for 90 minutes. The membrane was blocked on PBS containing 3% BSA overnight. The membrane was incubated with a rabbit anti-GFP mAb (Research Diagnostics Inc., Flanders NJ, USA) at a dilution of 1:5000 for 1h at room temperature, washed three times and then incubated with a peroxidase-labeled goat anti-rabbit Ab (Dianova, Hamburg, Germany) at a dilution of 1:10,000 for 1h at room temperature. The blots were developed with enhanced chemiluminescence (ECL). The ECL solution consisted of 10 mL ECL-A (0.25% (w/v) luminol in 1M Tris/HCl), 100 μ L ECL-B (0.11% (w/v) para-hydroxycoumarin acid in DMSO), and 3.1 μ L of 30% H₂O₂. Luminescence was documented using an autoradiography film (GE Healthcare).

16.9 IgG response to vaccines

The IgG responses to measles and rubella virus were measured by routine ELISA in the department of clinical chemistry of the LMU using the Enzygnost Anti-Rubella Measles Virus/IgG and Anti-Measles Virus/IgG assays (Siemens Healthcare, Erlangen, Germany).

Part V

Results

Parts of the following results were published in [Mayer *et al.* 2013].

17 Cloning and expression of MOG constructs with a C-terminal, intracellular EGFP tag

hMOG and mMOG were cloned into the pEGFP-N1 plasmid, yielding MOG constructs with a C-terminal EGFP tag. The hMOG-EGFP construct was then mutated as described in Material and Methods to achieve 7 mutants of hMOG with a C-terminal, intracellular, EGFP-tag (N31D, H103A/S104E, S104E, P42S, R86Q, R9G/H10Y and P42S/H103A/S104E). Similar extents of expression were obtained with the different constructs, as shown by comparable FL-1 intensities, reflecting EGFP-fluorescence (figure 9).

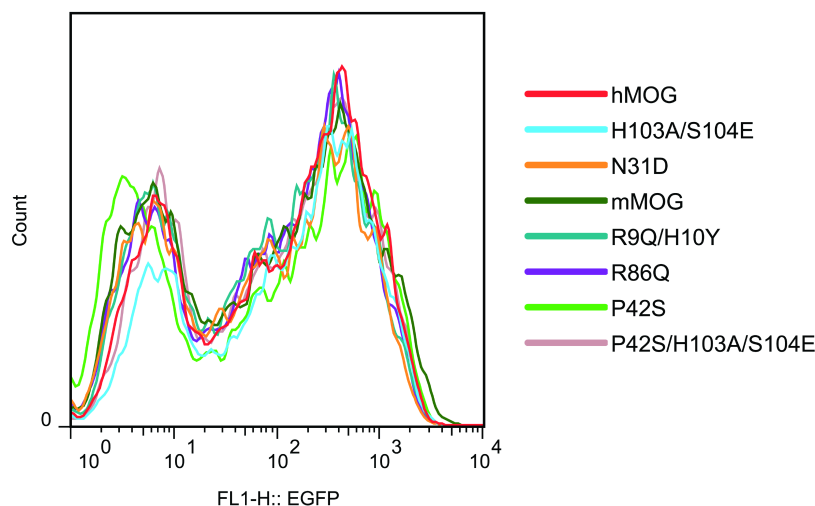


Figure 9: Expression intensity of the applied MOG variants. HeLa cells were transiently transfected with the indicated MOG-variant fused to EGFP. Depicted is the fluorescence intensity of the FL-1 channel (EGFP) of 8 different MOG mutants, measured 24h after transfection. Frequency and fluorescence intensity were comparable, allowing for comparison of binding to different mutants. The single mutant S104E is not shown in this figure, as this mutant was only tested for a subset of sera, as explained in section 20.1.

Surface expression of each MOG variant was evaluated with two anti-MOG mAbs, 8-

18C5 and Y11. These two mAbs were chosen because they recognize different epitopes on MOG [Breithaupt *et al.* 2008]. 8-18C5 did not recognize the three MOG variants containing the S104E mutation, but bound well to all other mutants. All MOG variants were recognized by Y11 (figure 10).

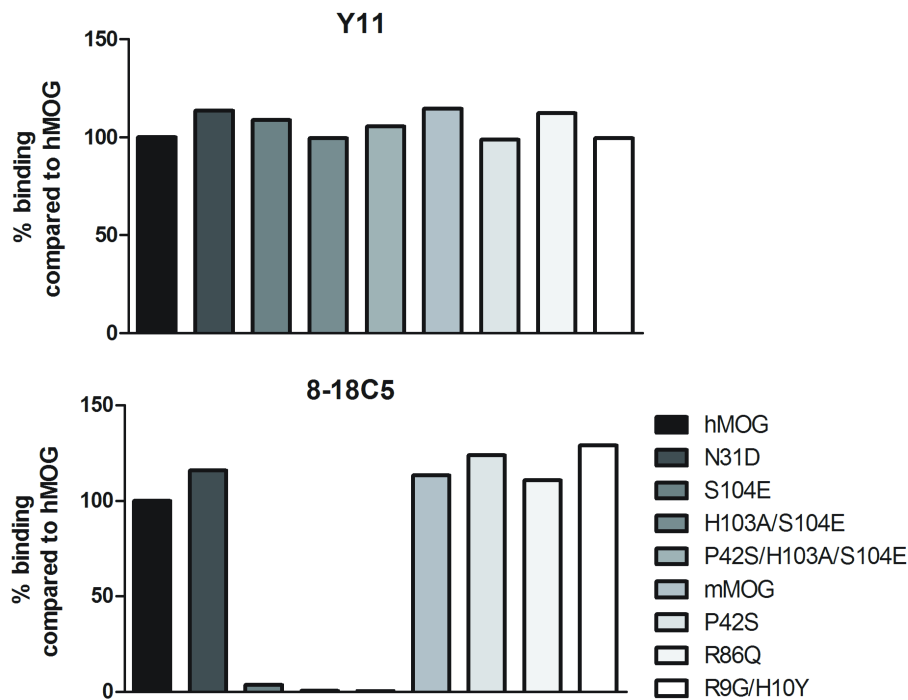


Figure 10: hMOG and all mutants were recognized equally by the anti-MOG mAb Y11 proving that they are correctly folded and expressed on the cell surface. In accordance with published data (Breithaupt *et al.*, 2008) the mAb 8-18C5 does not recognize MOG anymore when the mutation S104E is introduced.

This shows that the introduced mutations did not interfere with MOG surface expression. Further it was previously shown that the introduction of the H103A/S104E mutation did not disturb the overall structure of rat MOG [Breithaupt *et al.* 2008]. The P42S mutation is also unlikely to change the overall structure of MOG, as both proline and serine are found in different species at this position.

18 Validation of transiently transfected MOG variants and reproducibility of binding ratios

In order to quantify the recognition of MOG-EGFP mutants by human antibodies, it was important to ensure 1. comparability of expression levels between the MOG constructs and 2. reproducibility of the results between different experiments. Using MOG-EGFP fusion proteins allows for comparison of the expression levels. EGFP fluorescence is seen in the FL1 channel. Cells with the FL1 fluorescence intensity of 10^2 - 10^3 (figure 11) were gated to evaluate the binding to the respective transfected cell. This range was selected to ensure a high expression level and a good comparability between the transfectants. The calculation of the binding percentage is described in Material and Methods and in figure 11.

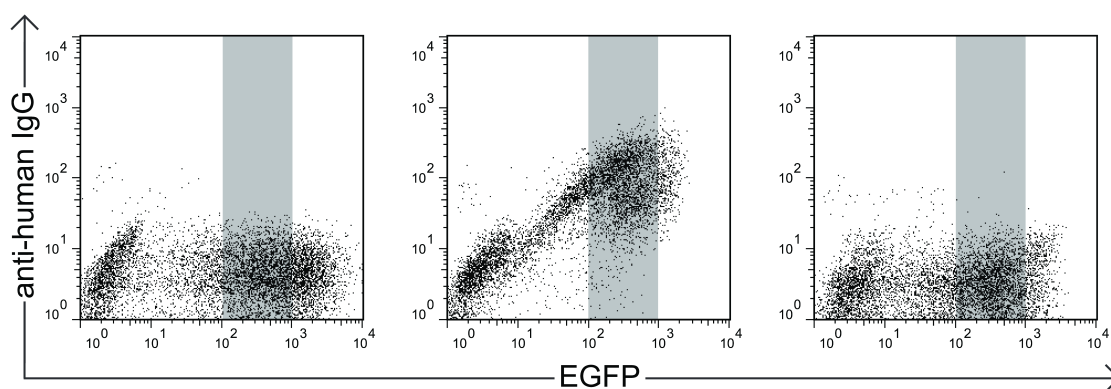


Figure 11: Processing of FACS data to calculate specific binding. Three different transfectants were stained with the same serum AEB085. Left: HeLa cells transfected with EGFP only (MCF FL-4= 4.47). Middle: HeLa cells transfected with hMOG- EGFP (MCF FL-4=79.7). Right: HeLa cells transfected with mMOG-EGFP (MCF FL-4=3.34). For binding calculation gates were set on the cells with an EGFP expression level between of 10^2 and 10^3 . Calculation of the binding percentage for the serum AEB085 shown above: AEB085 % binding of mMOG compared to hMOG = $\frac{(3.34-4.47)}{(79.7-4.47)} \times 100\% = -1.5\% \approx 0\%$.

The similar expression levels of the mutants, the gating on cells with a defined expression level (10^2 - 10^3), and the demonstration of binding of at least one MOG-specific mAb allowed the comparison of binding to the different mutants. In order to assess the

reproducibility of the system, binding of the 111 sera to the mutants was analyzed up to three times in independent experiments, yielding a very good reproducibility of the binding percentage: For 36 sera, recognition of the three most important constructs P42S, mMOG and H103A/S104E to hMOG (i.e. 108 measurements and each in triplicates) was analyzed, yielding following results: A) In 33/108 measurements the mutation reduced the binding to less than 10%, with an absolute SD of 7.8%. B) In the other 75 measurements, binding was either strongly reduced (i.e. below 65%), comparable to hMOG (i.e. between 65 and 200%) or strongly increased (i.e. above 200%); here the SD of the binding was 20% of the binding percentage. Representative sera analyzed three times are shown in figure 15. A subset of 16 sera was independently analyzed by Prof. Dr. Markus Reindl in Innsbruck for binding to P42S and mMOG by titration in an immunofluorescence assay using transiently transfected HEK-293A cells: the resulting 32 binding percentage values were very well comparable between the independent assays: Spearman $r=0.7136$, $p<0.0001$. This shows that the results are even reproducible in a different experimental setup.

19 Glycosylation of MOG-EGFP fusion proteins in HeLa cells

HeLa cells were transiently transfected with the different MOG-EGFP constructs, the lysates were digested with PNGaseF and the size of the digested and undigested fusion proteins were compared with a Western-blot in order to assess their N-glycosylation. Deglycosylation with PNGaseF yielded MOG-EGFP fusion proteins with the same size as the N31D mutant (figure 12), indicating that N31D is the only N-glycosylation site used in this setting.

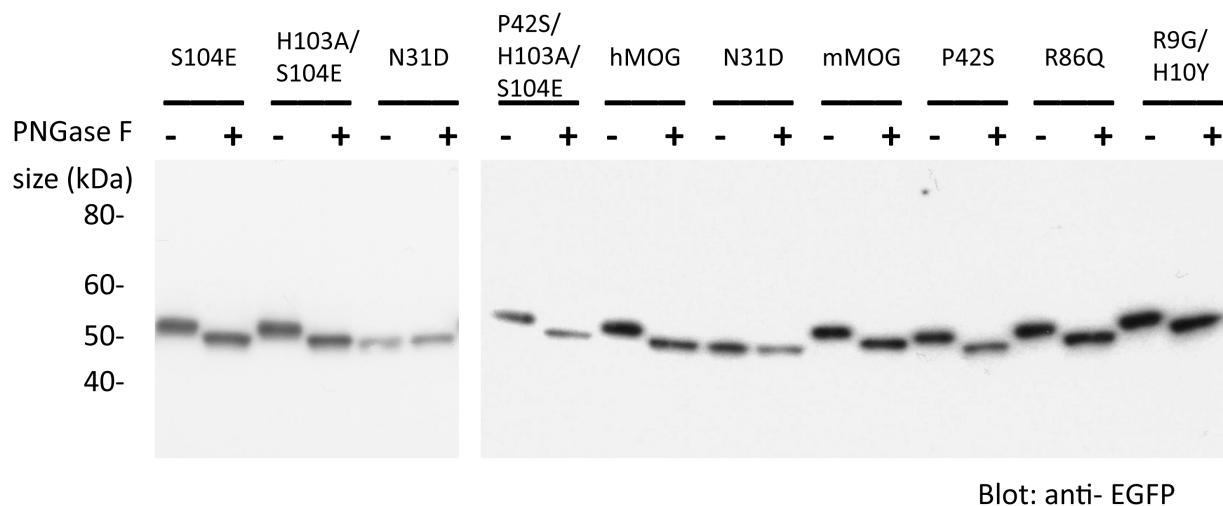


Figure 12: N31D mutation completely abrogates MOG-glycosylation. Cell lysates of HeLa cells transiently transfected with MOG-variants were digested with PNGase F as indicated; 6 mg total protein were loaded into each well of an SDS gel, separated by gel electrophoresis, blotted onto nitrocellulose, incubated with a rabbit anti-EGFP mAb and developed with a peroxidase-labeled goat anti-rabbit antibody and ECL. After digestion with PNGase F, all MOG-mutants had the same size as N31D. Digestion of N31D did not alter the size of this particular mutant.

20 Recognition of MOG-epitopes analyzed with single and multiple amino acid mutants

98/111 anti-MOG positive sera showed a reduced binding to at least one of the MOG variants. In 52/111 samples, the immune response was clearly reduced by mutations of amino acids positioned in only one loop. In 39/52 patients, binding to single mutated loops was decreased to less than one third, indicating that the IgG response is focused on one epitope. In 32/111, binding to multiple mutants was reduced and in 14/111 samples there was no binding to mMOG, but no specific responsible amino acid was identified. The responses to the described mutants allowed distinction of 7 different patterns of MOG recognition. The intensity of the recognition of hMOG did not differ significantly between sera recognizing the 7 patterns, as summarized in figure 14. The structure of MOG with the strands and loops referred to in this work is shown in figure 13. An overview of these patterns is shown in figure 14 and examples of the seven patterns are shown in figure 15.

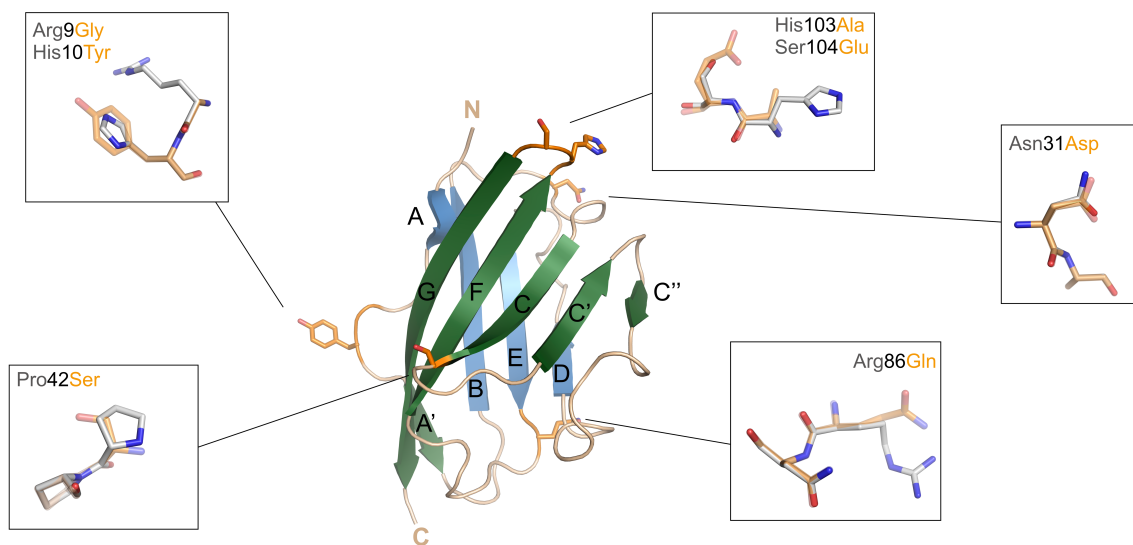


Figure 13: Structure of MOG and modeling of the epitopes recognized by human autoantibodies on MOG. This figure was taken from [Mayer *et al.* 2013] and was created by Dr. Constanze Breithaupt. MOG has an IgV like fold, which means it looks a bit like a sandwich formed by two slices of toast. The toast slices are called β -sheets (one is shown in green, the other one is blue), they are both made up of amino acid chains. These chains (called β -strands) run antiparallel to each other. The β -strands are connected to each other by loops, which also consist of amino acids. Residues at positions that were mutated in this study are shown as a stick model. Close-up views of these regions show the superposition of the side chains of hMOG (gray) modeled with SWISS-MODEL [Schwede *et al.* 2003] and the corresponding side chains of mMOG, the rMOG double mutant H103A/S104E [Breithaupt *et al.* 2008] and the modeled N31D mutation, respectively (orange).

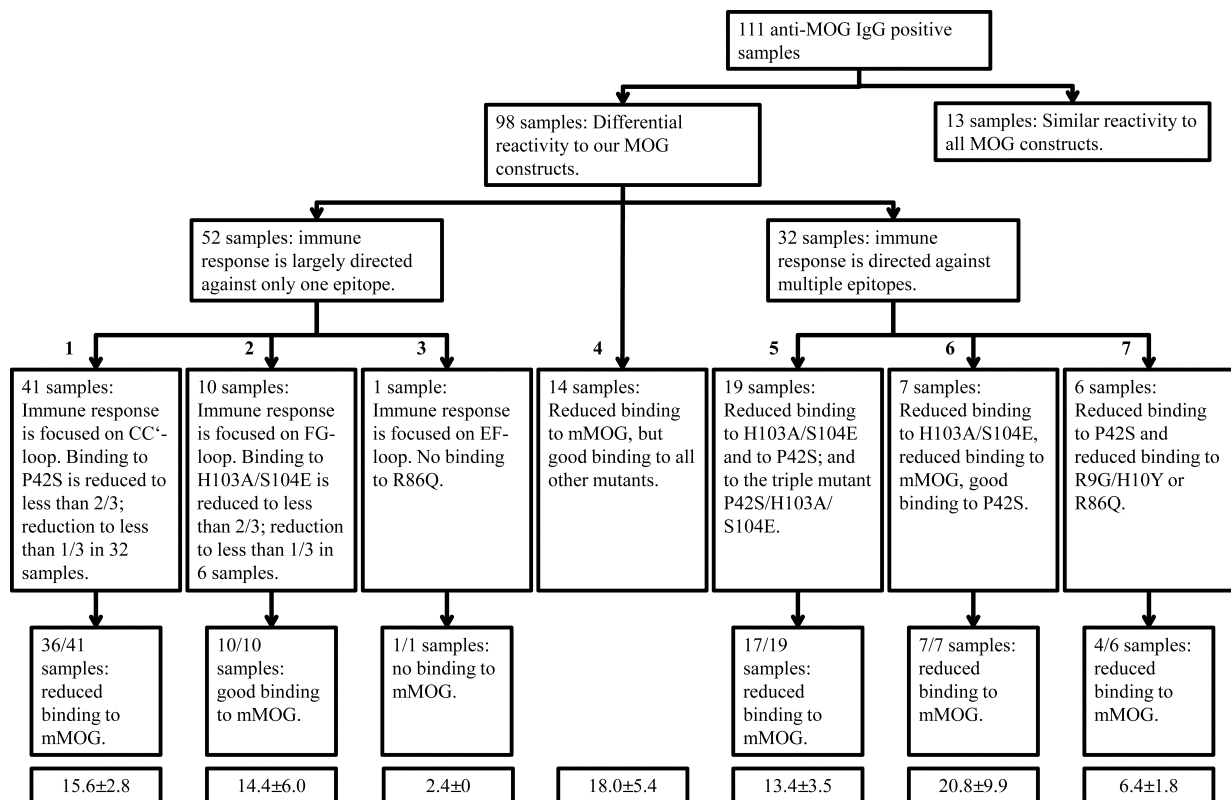


Figure 14: Anti-MOG reactivity grouped in seven patterns. The epitope recognition of 111 sera was analyzed using 9 MOG variants. Epitope patterns were assigned in 98 samples, which were grouped into seven patterns, indicated by the numbers 1–7 in row 4. Fifty-two of 98 samples showed an immune response focused on one epitope (patterns 1–3). Fourteen of 98 samples showed reduced binding to mMOG, but recognized all other mutants well (pattern 4). Thirty-two samples showed an immune response directed against multiple distant epitopes (patterns 5–7). In the last row, the intensity of the anti-hMOG reactivity of each pattern is indicated. The values shown are the FACS ratios (MCF reactivity to hMOG/MCF reactivity to EGFP; mean ± SEM). The anti-hMOG reactivity varied within each pattern, but did not differ significantly between the different patterns (difference between any two patterns, one-way ANOVA, $p > 0.05$).

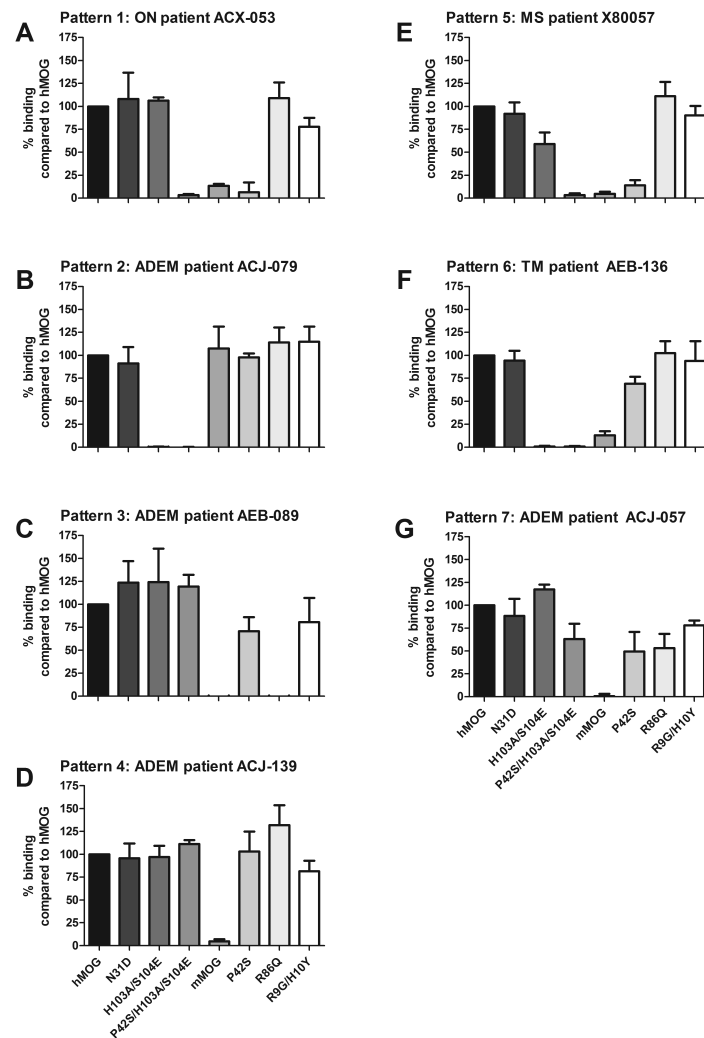


Figure 15: Examples of the seven identified epitope patterns of anti-MOG reactivity. Depicted is the mean percentage binding value of three independent experiments. Error bars represent the SD. In patterns 1–3 the anti-MOG IgG response is focused on only one epitope. In pattern 1, the anti-MOG response is directed against the CC'-loop of MOG, binding to P42S and to mMOG is reduced; binding to P42S/H103A/ S104E is also reduced. In pattern 2, the anti-MOG response is directed against the FG-loop of MOG; this causes a reduction in binding to H103A/S104E and to P42S/H103A/S104E. In pattern 3, the anti-MOG response is directed against the EF-loop of MOG. Binding to R86Q and to mMOG is reduced. In pattern 4, binding to mMOG is reduced, but the mutations P42S, R86Q, and R9G/H10Y introducing individually the murine amino acids had no effect on binding. The immune response of patients recognizing patterns 5–7 is directed against multiple distinct epitopes. In pattern 5, the anti-MOG response is directed against the FG-loop and the CC'-loop of MOG. Binding to H103A/S104E, P42S/ H103A/S104E, mMOG, and P42S is reduced. In pattern 6, binding to H103A/S104E and to mMOG is reduced; the mutations P42S, R86Q, and R9G/H10Y had no effect on binding. In pattern 7, binding was directed against the CC'- loop (reduced binding to P42S) and to a second loop, either the EF-loop (reduced binding to R86Q) or the AA'-loop (reduced binding to R9G/H10Y).

20.1 Patients with anti-MOG IgG directed to one epitope

The most frequently recognized MOG-epitope was revealed by the P42S mutation positioned in the CC'-loop (figure 6). 66/111 patients (59%) showed a reduced or no binding to this mutant (patterns 1, 5 and 7). Moreover, in 41/111 patients (37%) the MOG-specific Ab response was focused on the CC'-loop (pattern 1, figure 15A). 36 of these 41 sera also showed reduced or no binding to mMOG, which was expected, since mMOG contains S42. In 21 of these 36 cases, binding to mMOG was lower than binding to P42S indicating that other differences between human and murine MOG further decreased binding to mMOG. The CC'-loop is hence identified as the most frequently recognized epitope on hMOG and as the dominant epitope in patient sera recognizing a single epitope. The tip of the FG-loop (which is the main target of anti-MOG mAbs) is recognized by 36/111 (32%) patients. In a subgroup of 10 patients (9%) the immune response is strongly focused on this region (pattern 2, figure 15B). These sera showed reduced or no binding to the double mutant H103A/S104E but bound well to the other mutants (P42S, R9G/H10Y, R86Q, N31D and mMOG). Comparing the reactivity of these 10 sera to the single mutant S104E and to the double mutant H103A/S104E revealed heterogeneity in recognition of the FG-loop: In 8/10 sera, reduced recognition of both the single mutant S104E and the double mutant was reduced, reminiscent of the binding pattern of the mAb 8-18C5. However, one other serum showed no decrease in binding to S104E, whereas one serum showed strongly increased binding to S104E, but not to H103A/S104E (data not shown). To analyze whether binding to the double mutant H103A/S104E and the single mutant S104E was comparable, 76 sera were measured with both mutants. These sera showed either decreased (34 sera binding less than 65%) or good recognition (42 sera) of H103A/S104E. Recognition of these two mutants was very similar (figure 16). This figure shows also that some sera bind better to these mutants than to the hMOG.

One serum did not bind the R86Q mutant anymore (pattern 3, figure 15C) and hence

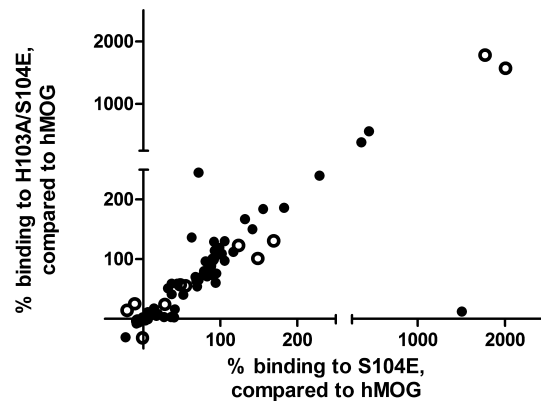


Figure 16: Binding to the double mutant H103A/S104E in comparison to the single mutant S104E. Binding to H103A/S104E was decreased (to less than 65%) in 34 of all sera. For these 34 and additional 42 sera binding well to H103A/S104E (76 in total) recognition of the single mutant S104E was also assessed. Depicted are the binding percentages for the 76 sera. Sera with low reactivity to hMOG (FACS ratio below 2.0) are depicted as open circles. The correlation was highly significant (Spearman $r = 0.85$, $p < 0.0001$). One ON patient recognized S104E with 1506% binding, but did not recognize the double mutant H103A/S104E.

recognized the EF-loop of MOG (figure 6). This serum also did not bind mMOG, as expected, since mMOG contains Q86. This serum recognized all other mutants well. For 14/111, we found a reduced recognition of mMOG, but were not able to identify the precise recognized epitopes (pattern 4, figure 15D). These anti-MOG antibodies might target regions with rather conservative mutations (C'D-loop or DE-loop, see figure 6) or their binding might be influenced by subtle structural differences that cannot be mimicked by the chosen mutants. In summary, the immune response was directed against one single epitope in 52/111 sera. The most frequently found single epitope is dominated by P42 that is not found in mMOG. The major mAb epitope located at the FG-loop is conserved between mMOG and hMOG and is the second most frequently recognized epitope in humans.

20.2 Patients with anti MOG IgG recognizing multiple epitopes

Reduced binding to multiple mutants was observed in 32/111 (29%) patient samples. The most common combination, present in 19 of 32 samples, was reduced binding to P42S and

to H103A/S104E (pattern 5, figure 15E). These mutations are located in loops at opposite ends of the A'GFCC'C'' β -sheet of MOG. The average distance of the C α atoms was determined by Dr. Constanze Breithaupt as distance of C α atoms: $d_{\text{average}} = 23\text{\AA}$). The observed maximum dimensions of Ab epitopes are $21\text{\AA} \times 28\text{\AA}$ [Ramaraj *et al.* 2012]. As exemplified by the MOG Igd (8-18C5) Fab complex structure in which the FG-loop forms the center of the epitope whereas S42 is located too far away to interact with antibody amino acids, P42 and H103/S104 cannot simultaneously bind to the center of an antibody paratope. Indeed, in 64/111 (58%) patient samples antibodies recognize either P42 (pattern 1, 7) or H103/S104 (pattern 2, 6). For this reason, sera showing pattern 5 reactivity can be assumed to contain at least two different antibody populations recognizing distinct epitopes. 4 of these 19 samples, however, showed strongly reduced binding (<10%) to both H103A/S104E and to P42S. This indicates that in these sera both loops influence antibody binding simultaneously. Considering the observed maximum dimensions of antibody epitopes and the distance between the two MOG loops, the epitopes recognized by these samples have to be very extended with hot spots of binding in the two loops at the edges of the epitope. In 7/111 patient samples, binding to H103A/S104E and to mMOG was reduced or abolished, but recognition of P42S and R9G/H10Y and R86Q was good (pattern 6, figure 15F). In 6/111 samples, binding was reduced to the P42S mutant and to the R9G/H10Y or to the R86Q mutant (pattern 7, figure 15G). We noted that sera showing pattern 7 reactivity, differ in reactivity to mMOG (binding to mMOG was reduced in 4/6) indicating that within this pattern further epitopes are recognized to different extents. Taken together, a subset of 32/111 sera showed reduced reactivity to various MOG constructs carrying distant mutations. In paragraph 20.1 it was described that the most frequently recognized epitopes are found at the CC'-loop and at the FG-loop of hMOG. In addition, the reactivity to both of these two epitopes is the most common combination among sera recognizing multiple epitopes.

20.3 The triple mutant P42S/H103A/S104E

Binding to the triple mutant P42S/H103A/S104E, which combined the two most important epitopes of human anti-MOG IgG, was reduced in 64% of all sera. As expected, all 19 sera that showed a reduced binding to both P42S and H103A/S104E showed strongly decreased binding to the triple mutant (less than 35% binding) (pattern 5, figure 15E). Within the group of 41 samples that recognized the immunodominant P42 (pattern 1), 13 showed increased, i.e. more than 200%, binding to H103A/S104E. 9 of these 13 sera also showed reduced binding to the triple mutant P42S/H103A/S104, while the other 4/13 bound this triple mutant comparably strong as hMOG (also see 20.5). Thus, the triple mutant revealed a further heterogeneity of sera recognizing the immunodominant P42. The triple mutant also allowed to further differentiate those sera that recognize the second most important epitope, the FG-loop. Within the subgroup of 17 sera with decreased binding to H103A/S104E (patterns 2 and 6), four sera showed increased binding to P42S. The one serum with pattern 6 recognition and a strongly increased P42S recognition showed poor recognition of mMOG. This could be explained by other more subtle structural differences between human and mMOG. In only 1 of these 4 sera, binding to the triple mutant was decreased. The remaining 3 sera bound well to the triple mutant. One example is the ON serum AEB048 that showed only 12% binding to H103A/S104E (pattern 2). This serum recognized P42S very well (2057% binding to P42S and 1518% binding to mMOG, compared to hMOG). In this case, binding to the triple mutant was not reduced, but was also stronger than to hMOG (610%). Taken together, sera with decreased reactivity to both P42S and to H103A/S104E also showed decreased reactivity to the triple mutant P42S/H103A/S104E. 13 sera with increased reactivity to H103A/S104E did not recognize P42S. In 9/13 cases, these autoantibodies did not recognize the triple mutant. Four sera showed increased reactivity to the P42S mutant. In 3/4 sera, these autoantibodies also bound the triple mutant well, although they did not recognize H103A/S104E.

20.4 The N31D mutant

The “no glycosylation” mutant N31D did not significantly lower anti-MOG recognition in any of the sera. Examples of recognition of N31D are shown in figures 15, 20 and 22. This proves that the glycosylated part of MOG is not recognized by autoantibodies. Instead, 8 sera recognized the unglycosylated MOG better than the hMOG (see 20.5). Five of these patients showed low recognition of hMOG, with a FACS ratio below 2.0. Enhanced recognition of the unglycosylated mutant was not linked to recognition of a certain epitope pattern (3/8 recognized pattern 4, 2/8 pattern 1; 1/8 pattern 2; 1/8 pattern 7 and one bound well to all mutants).

20.5 Higher reactivity to mutated variants of MOG

32/111 patients showed a clearly elevated (more than two fold) reactivity to mutated variants of MOG as compared to hMOG. Some bound multiple mutants better than hMOG. These 32 patients include 8 recognizing MOG better in the absence of glycosylation (N31D mutant, details in 20.4). 12 patients recognized mMOG better than hMOG, 6 of these also bound better to P42S than to hMOG. This increase in binding to P42S might be explained by the rigidity of proline and the flexibility of serine, allowing an induced fit of the protein to the antibody. For 6/12 patients with high reactivity to mMOG, no epitope recognition pattern could be assigned; 3/12 showed pattern 2 recognition and 3/12 recognized other patterns. 17/111 patient sera bound H103A/S104E better than hMOG, 4 of which also bound better to mMOG; 13 of these 17 sera recognized pattern 1 (reduced binding to P42S). 9/13 sera with increased binding to H103A/S104E and pattern 1 recognition (reduced binding to P42S) also showed reduced binding to the triple mutant P42S/H103A/S104E, as described in 20.3. As explained in 20.2, these sera could contain at least two different kinds of anti-MOG antibodies- one recognizing the CC'-loop and one other with improved binding to the artificial mutant H103A/S104E. However it seems that

an antibody recognizes both loops simultaneously at the edge of the epitope. Another possible explanation for increased recognition of MOG variants could be that high affinity anti-MOG antibodies do not recognize a MOG variant and hence allow lower affinity anti-MOG antibodies to bind. Theoretically, the sum of binding of these low-affinity antibodies could result in an increased FACS ratio. Taken together, a subset of 32/111 sera showed increased reactivity to mutated variants of MOG. The most common mutants to elevate autoantibody binding were H103A/S104E, mMOG and N31D.

20.5.1 The S104E mutation could mimic phosphorylated MOG

The glutamate mutation leads to a negative charge at this position, which is not present in the wildtype variant of hMOG. This negative charge is reminiscent of phosphoserine. For this reason, it was analyzed, using the phosphorylation prediction program NetPhos 2.0 [Blom *et al.* 1999], whether this particular serine residue is a likely site for phosphorylation. With a score of 0.994, S104 is a very likely phosphorylation site (see figure 17).

20.6 Serial dilution of two sera showing differential recognition to MOG variants

Sera of an adult ADEM patient 18078 and a pediatric TM patient (mono ADS) AEB-123 were serially diluted in 1:4 steps up to a dilution of 1/12800. The adult ADEM patient 18078 showed pattern 7 recognition with increased recognition to H103A/S104E (as described in 20.5). As shown in figure 18, binding to hMOG was seen up to a dilution of 1/200, while binding to H103A/S104E was seen up to a dilution of 1/800. The decreased recognition of P42S and mMOG is also seen at a dilution of 1/200. The pediatric TM patient AEB-123 showed pattern 1 recognition. As shown in figure 18, the binding patterns of this patient was seen up to a dilution of 1/3200. These results show that the binding patterns are dose-independent.

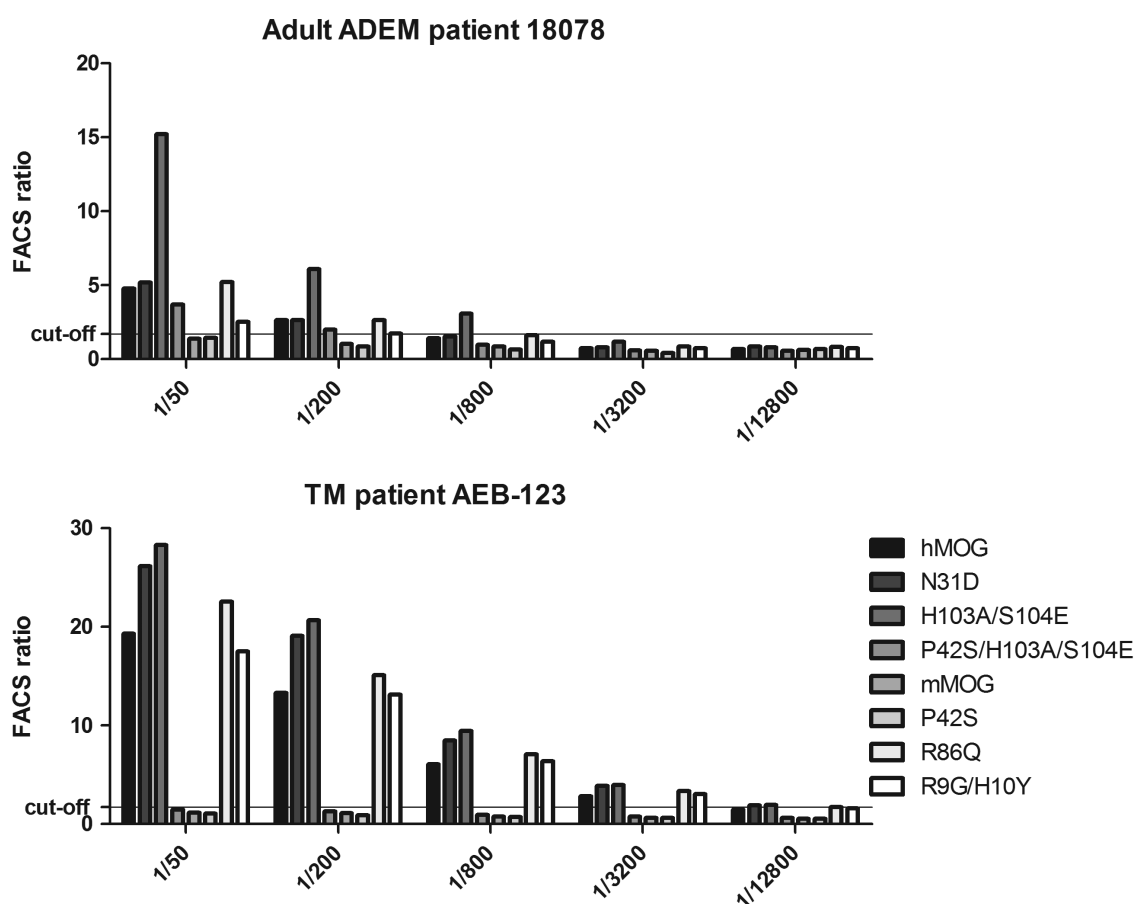


Figure 18: Serial dilution of two sera with differential recognition of MOG variants. The adult ADEM serum 18078 showed enhanced recognition of the H103A/S104E mutant and did recognize mMOG and the P42S mutant. Recognition of the R9G/H10Y mutant was reduced. This pattern was seen at a dilution of 1/50 and 1/200. At a dilution of 1/800, only binding to the H103A/S104E mutant was above the cut-off, reflecting the increased recognition of this mutant. The pediatric TM (mono ADS) serum AEB-123 did not recognize P42S/H103A/S104E, mMOG or P42S. This pattern was seen up to a dilution of 1/3200. At a dilution of 1/12800, recognition of hMOG was slightly below the cut-off.

21 Comparison of MOG epitope analysis with mutated variants versus competition with defined mAbs

A commonly used method to analyze epitope recognition is competition with mAbs. This technique has also been used to analyze the epitopes recognized by human anti-MOG antibodies [McLaughlin *et al.* 2009, Proebstel *et al.* 2011]. The single amino acid mutation assay was compared to blocking assays with defined mAbs. The mAbs 8-18C5 and Y11 recognize different epitopes on MOG [Breithaupt *et al.* 2008]. IgG binding of 15 sera in competition with either 8-18C5 or Y11 was analyzed; both mAbs competed with the human IgG in 15/15 sera. The tested sera recognized different epitopes, 13 of them recognized patterns 1, 2, 4, 5, 6 and 7 and two bound well to all mutants. Figure 19 shows two sera that were blocked by the mAbs 8-18-C5 and Y11 to a similar extent, although they recognized different epitopes as revealed by the MOG mutants; the mutation H103A/S104E abrogated the binding of one, but did not interfere with the binding of the other serum. This shows that mAbs can block binding of human anti-MOG IgG, even when a different epitope is recognized by the human antibodies. Hence, systematic mutation of amino acids gives more detailed information about the epitopes recognized by human anti MOG antibodies than competition assays with defined mAbs.

22 MOG epitopes recognized by patients with different disease entities

A linkage between epitope recognition and diagnosis has been shown for antibodies against heat shock proteins 60 and 65: patients with inflammatory bowel disease and coronary heart disease and healthy controls each recognized different epitopes [Fust *et al.* 2012]. For this reason, it was assessed whether anti-MOG antibody epitopes also differ between the

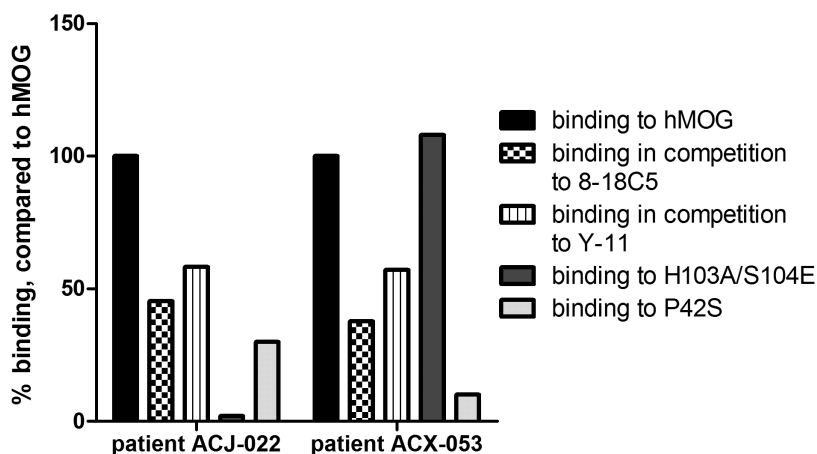


Figure 19: Mutated variants of MOG allowed more precise insight into recognized epitopes than blocking with mAbs. The two patient sera displayed here showed a different reactivity to mutated variants of MOG: ACJ-022 recognized the FG-loop containing H103/S104 and the CC'-loop containing P42S (pattern 5); ACX053 did not bind the FG-loop, but recognized the CC'-loop containing P42 (pattern 1). Nevertheless, both sera were blocked by the two anti-MOG mAbs 8-18C5 and Y11 to a similar extent. The mAb 8-18C-5 recognizes the FG-loop of MOG [Breithaupt *et al.* 2008]. Y11 binds cell-bound MOG and the hMOG peptide aa76-100 [Brehm *et al.* 1999].

analyzed patient groups. Distinct epitope patterns are recognized by anti-MOG antibodies in the serum of patients with 6 different clinical entities: ADEM, mono ADS, MS, CRION, NMO and other relapsing ADS cases. Each epitope pattern was found in several clinical presentations, as summarized in table 7. No statistically significant association between epitope recognition and diagnosis was found (Chi square test, $p=0.27$). Nevertheless, a larger sample size might potentially reveal such an association. It is interesting to note that in the CRION group, 4/10 and only 4/101 other patients showed more than 200% binding to the N31D mutant. We analyzed whether patients with chronic inflammatory diseases had an anti-MOG response directed against more epitopes than patients with a monophasic disease. Out of 26 cases of chronic inflammatory diseases namely MS, NMO, CRION and other relapsing ADS cases, 35% recognized multiple epitopes (patterns 5, 6 and 7) and 31% a single epitope (patterns 1, 2 and 3). Out of 85 patients with a monophasic disease (ADEM and mono ADS), 27% recognized multiple epitopes (patterns 5-7) and

44% recognized a single epitope (patterns 1-3). These results are summarized in table and indicate that recognition of a single or of multiple epitopes is not linked to monophasic or chronic disease.

Disease	No. of patients	Pattern 1	Pattern 2	Pattern 3	Pattern 4	Pattern 5	Pattern 6	Pattern 7	No Epitope Found
Mono ADS other than ADEM	45	18	4	0	4	8	2	2	7
ADEM	40	16	5	1	5	5	3	3	2
MS	10	3	0	0	1	2	1	0	3
NMO like	2	0	0	0	0	1	1	0	0
CRION	10	3	1	0	4	0	0	1	1
Other relapsing ADS	4	1	0	0	0	3	0	0	0

Table 7: Recognition of epitope patterns in different disease groups

23 Long term analysis of individual epitope patterns on MOG

In order to analyze the temporal stability of individual epitope patterns, follow-up sera of 11 anti-MOG antibody positive patients were analyzed with the different MOG-constructs. For 9/11 one of the above mentioned epitope patterns was assigned. The patterns stayed constant in 9/9 analyzed cases for an observation period of up to 50 months (MS) without evidence for intramolecular epitope spreading (figures 20 and 22). Constant epitope patterns were found in MS, CRION and ADEM. This was especially remarkable for MS patients. In pediatric MS patients, anti-MOG IgG persists with fluctuations [Proebstel *et al.* 2011]. For example, the anti-MOG reactivity of the MS patient ACJ-162 (figure 22H) decreased below detection level after 12 months, but clear anti-MOG reactivity was seen after 24 months. Here, the anti-MOG antibodies still recognized the same pattern (pattern 1) after a follow-up period of 36 months. Different epitope patterns, 1, 2, 4, 5, 6 and 7, stayed constant over years.

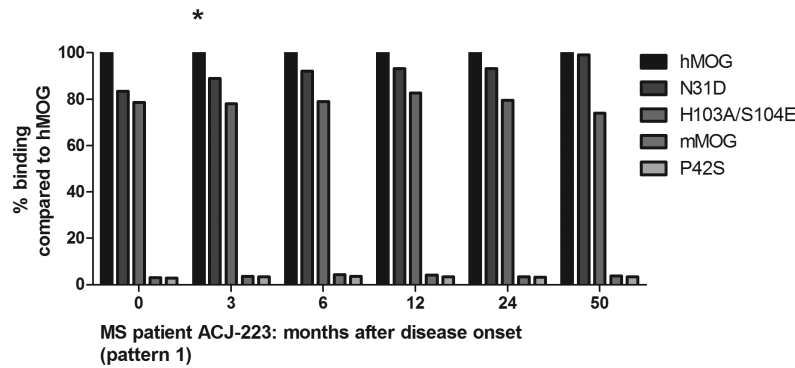


Figure 20: Temporal stability of recognition of MOG-epitopes. Depicted is a case of pediatric MS with a pattern 1 recognition. The recognition pattern stayed constant over the observation period of 50 months. An increased recognition of hMOG after three months is marked with an asterisk.

24 Comparison of the dynamic of anti-MOG IgG with anti-measles virus and anti-rubella virus IgG

Anti-MOG antibodies in patients with a monophasic disease course rapidly lose their anti-MOG antibodies [Proebstel *et al.* 2011]. In order to assess, whether these patients are generally incapable of producing a long-lasting IgG response, three patients with a rapid decline of anti-MOG IgG were selected. All three patients had been vaccinated against measles and rubella virus, IgG against these vaccines typically persist. All three patients mounted a persisting IgG response against both measles and rubella virus, while they rapidly lost the anti-MOG IgG (figure 21). This shows that the rapid loss of anti-MOG IgG in these patients is not linked to a general incapability of producing a long-lasting IgG response.

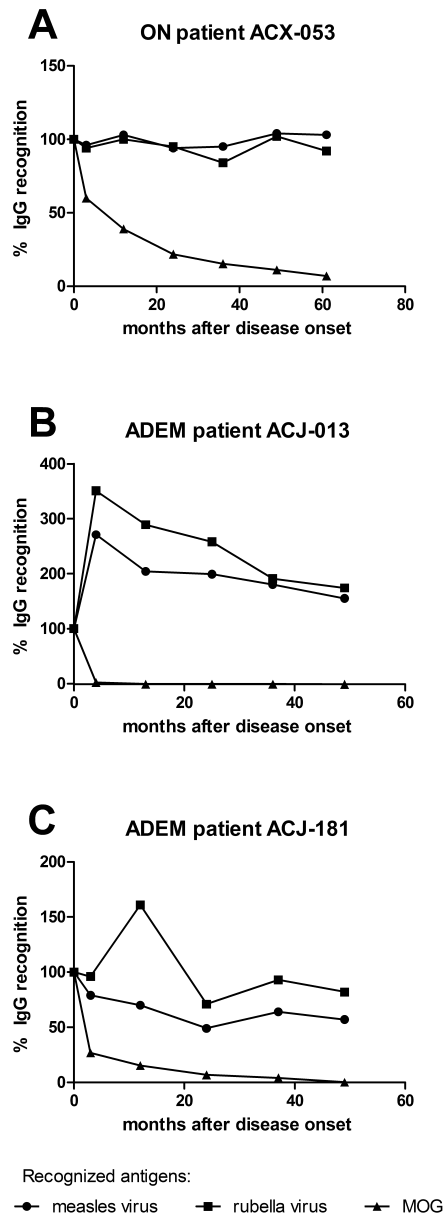


Figure 21: Dynamic of anti-MOG IgG compared with anti-measles virus and anti-rubella virus IgG. The IgG recognition of measles virus, rubella virus, and MOG was analyzed for an observation period of up to 60 months. The response at disease onset was set as 100% for each antigen and the subsequent responses were calculated. In these three patients, IgG against MOG declined quickly, whereas the IgG response against measles and rubella virus vaccine was stable for the observation period of 5 years. All three patients had a monophasic CNS inflammation. (A) Patient ACX-053 experienced a single episode of optic neuritis. (B and C) Patients ACJ-013 and ACJ-181 had monophasic ADEM.

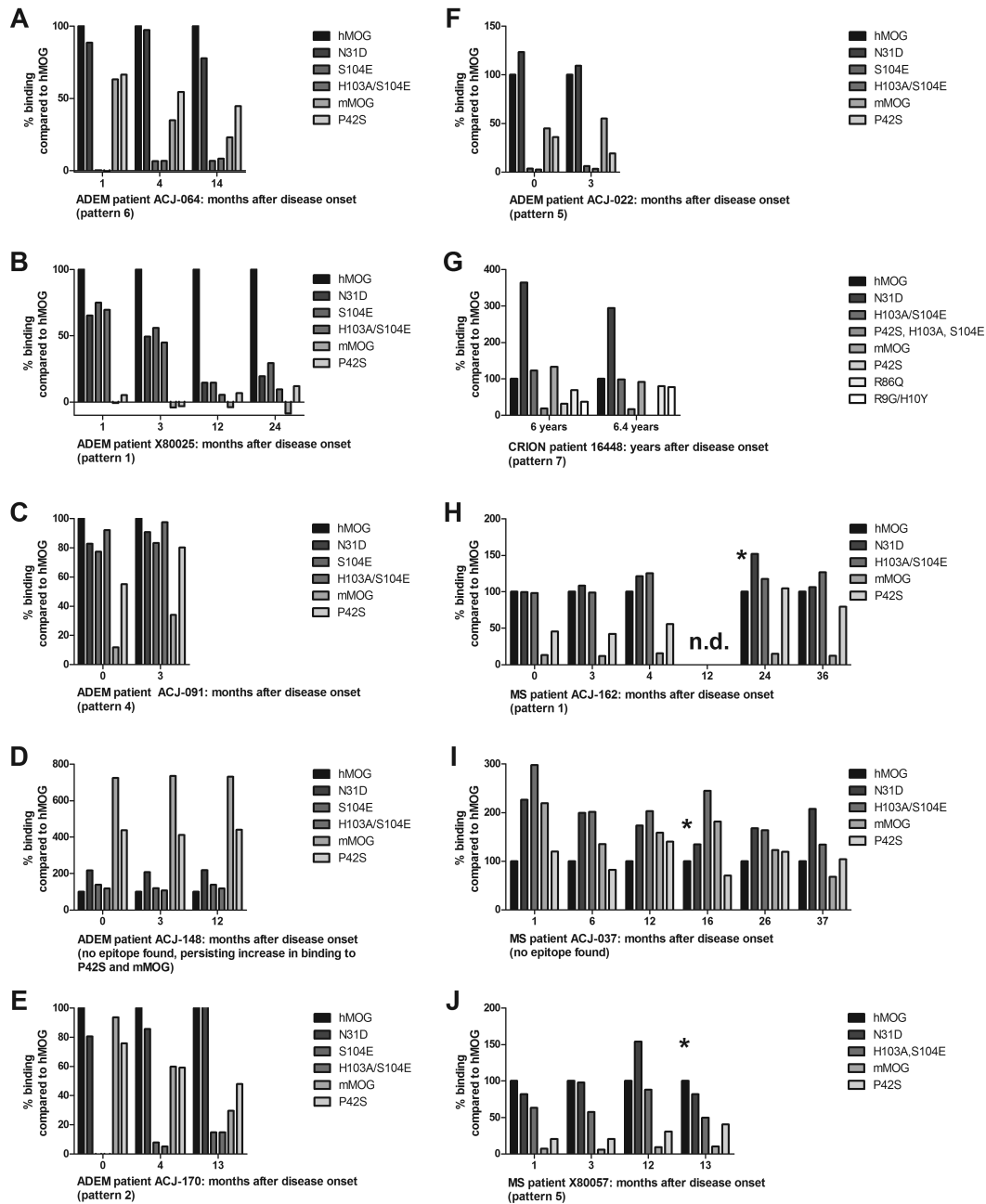


Figure 22: Temporal stability of recognition of MOG-epitopes. Ten sera were longitudinally analyzed for their epitope recognition (additional to figure 20). The observation period was up to 37 months (I). The patients had different diseases, namely ADEM (A-F), CRION (G) and MS (H-J). Anti-MOG reactivity showed a second increase in all examined MS sera [Proebstel *et al.* 2011] and the time point of the increase is labeled with a star (*). In the MS serum ACJ-162, the anti-MOG IgG fell below the detection limit at 12 months (n.d., not detectable), but reappeared at 24 months. Despite these fluctuations in the intensity of anti-MOG reactivity, the epitope recognition patterns stayed constant. The CRION patient experienced her 11th and 12th episode of optic neuritis.

Part VI

Discussion

25 The polyclonal anti-MOG response is directed against amino acid loops

In this work, 9 variants of MOG were expressed on the cell surface of HeLa cells with an intracellular EGFP-tag. 111 sera with MOG antibodies, collected from patients with different inflammatory CNS diseases, were analyzed for the recognition of these mutants. All epitopes identified in this work are located at loops that connect the β -strands of the IgV-like fold of MOG. This observation is in harmony with the concept that antigenicity correlates with solvent accessibility and flexibility in proteins [Thornton *et al.* 1986]. It is currently unknown whether the serum anti-MOG antibody response is polyclonal. This work provides direct evidence for the polyclonality of at least a subgroup of anti-MOG sera, because binding to multiple mutants was reduced in about a third of all donors. To further analyze the clonality of these antibodies, isoelectric focusing, with subsequent Western blotting of the purified anti-MOG antibodies could be performed, similar to Western blots used for the analysis of oligoclonal bands.

26 Species specific recognition

Most of the patients recognizing hMOG did not recognize mMOG, largely because the majority of sera did not bind to P42S, which is also found in mMOG. Other amino acid differences between the two species also contribute to the differential recognition of human and murine MOG (patterns 3, 4, and 7). The recognized proline at position 42 is also not present in rats, not even in the New World primate *Callithrix jacchus*, but appears in the rhesus monkey (*Macaca mulatta*). This species specific recognition pattern is different from the features of anti-AQP4 autoantibodies. Human anti-hAQP4 antibodies cross-react with mAQP4; staining of mouse tissue was even used to identify NMO IgG [Lennon *et al.* 2004]. This study shows that other human autoantigens might be missed when screening with

rodent tissue and even primate tissue might cause troubles.

27 Expanding the model of hMOG

Although human MOG has not been crystallized, crystal structures of mMOG [Clements *et al.* 2003] and rMOG [Breithaupt *et al.* 2003] have been published. The overall dimensions of the extracellular domain of MOG are $40 \times 35 \times 30 \text{ \AA}$ [Clements *et al.* 2003]. The observed maximum dimensions of Ab epitopes are $21 \text{ \AA} \times 28 \text{ \AA}$ [Ramaraj *et al.* 2012]. As shown in figure 6, only 11 amino acids differ between the extracellular domains of human and mMOG. Yet, the recognition of human anti-MOG IgG was dramatically reduced to mMOG (see 26), with P42S having the strongest impact on antibody recognition. This shows that this one difference between human and rodent MOG significantly changes the surface properties of MOG at this position, even though the C α atoms are predicted to be at the same positions, as shown in figure 23.

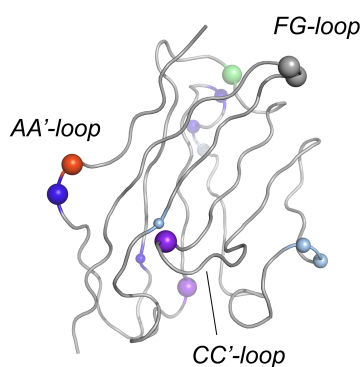


Figure 23: Sequence conservation of mMOG and hMOG mapped onto the three-dimensional structure of mMOG. Selected residues are displayed in three different sizes. C α -atoms of residues mutated in this study are shown as largest spheres: R9G/H10Y in red and blue, N31D greenish, H103A/S104E in gray, and P42S and R86Q in purple. C α -atoms of nonconserved residues, which were not mutated in this study, are shown as mid-sized spheres: G59A/D60E, D74E/A75T, and G77S. These C α -atoms are displayed in blue, indicating conservative amino acid differences between mMOG and hMOG. C α -atoms of nonconserved residues with side chains located inside the protein are shown as small spheres: V20A and F96Y.

28 Pathogenicity of anti-MOG antibodies in humans

The pathogenic potential of human autoantibodies is best demonstrated by the transfer of these antibodies into experimental animals as done with anti-AQP4 antibodies [Bennett *et al.* 2009, Bradl *et al.* 2009, Saadoun *et al.* 2011, Kinoshita *et al.* 2009]. Human antibodies to MOG have all the characteristics of pathogenic autoantibodies: they recognize MOG in its correct conformation, they are mostly of the complement fixing isotype IgG1 [Mader *et al.* 2011, Proebstel *et al.* 2011, McLaughlin *et al.* 2009], and they activate antibody dependent cellular cytotoxicity [Mader *et al.* 2011, Brilot *et al.* 2009]. Their pathogenic activity, however, has not yet been shown with affinity-purified antibodies. Transfer experiments with concentrated human sera [Zhou *et al.* 2006] are difficult to interpret, because human sera could have pathogenic compounds beyond anti-MOG IgG. Only a minority of human sera with anti-MOG IgG are suitable for transfer experiments in mice. The major autoantibody epitope found here is different from the immunodominant and pathogenic epitope in rodents [Breithaupt *et al.* 2008]. Human anti-MOG antibodies mainly recognized the CC'-loop containing P42 of hMOG, whereas most mouse mAbs to MOG recognized the FG-loop. Animal experiments have shown that not all antibodies against MOG are pathogenic [Brehm *et al.* 1999, Marta *et al.* 2005, Bjiçedingen *et al.* 2002]. Mouse mAbs, which recognize MOG on the cell surface and are pathogenic, can recognize different epitopes: both the mAb 8-18C5 and the mAb Y11 are pathogenic [Piddlesden *et al.* 1993]. Thus, one would expect that not only those human anti-MOG antibodies recognizing the FG-loop (patterns 2, 5, and 6), but that also other antibodies recognizing another part of the surface of MOG, e.g., the CC'-loop, are pathogenic. The CC'-loop is closer to the membrane than the FG-loop. Because this loop is recognized by antibodies when displayed on the surface of transfected cells, it is most likely also recognized on the surface of myelin. It is evident from features of the anti-MOG mAb Y11 that the same Ab can recognize both a linear peptide and the cell-bound con-

formationally intact MOG protein [Brehm *et al.* 1999]. Thus, it is likely that some of the anti-MOG antibodies in patients recognizing cell-bound MOG also recognize linear peptides. In the CNS, binding to a MOG peptide in solution, e.g. in the context of cell death, will not cause complement fixation, but might contribute to clearance by macrophages via Fc-receptors.

29 Assay comparison and evaluation

This study shows that the application of mutant variants of MOG allows a more precise insight into epitope recognition than blocking with defined mAbs does. In agreement with previous studies, the anti-MOG mAb 8-18C5 competes with binding of human antibodies to cell-bound MOG [McLaughlin *et al.* 2009, Proebstel *et al.* 2011]. This mAb also inhibits sera recognizing different epitopes. This is not surprising, because MOG is a relatively small protein, with only 125 extracellular amino acids [Kroepfl *et al.* 1996]. At the outermost periphery of the epitope, R52 of the 8-18C5 H chain contacts the MOG amino acids Y40 and S45 [Breithaupt *et al.* 2003], making clashes with antibodies that bind the nearby amino acid 42 to the center of their paratope highly likely. For this reason, binding of a mAb can inhibit binding of anti-MOG autoantibodies, even if they recognize different distant loops of MOG. Therefore, specific mutation of single amino acids gives a much more detailed and correct insight into epitope recognition, whereas competition analysis might be misleading. Similar results were found for anti-acetylcholine receptor (AChR) autoantibodies. Anti-AChR mAbs compete with human autoantibodies [Tzartos *et al.* 1982]. Further epitope mapping revealed that some human anti-AChR autoantibodies recognized different epitopes than the competing mAbs; the area covered by one single mAb was large enough to allow blocking of human autoantibodies recognizing distant epitopes [Luo *et al.* 2009]. This study analyzes epitopes of human anti-MOG antibodies with mutated cell-bound MOG. Earlier studies using peptide ELISA assays

[Xu *et al.* 2012, Haase *et al.* 2001, Khalil *et al.* 2006] would not give information on epitopes of conformationally intact MOG. This work shows that human anti-MOG antibodies recognize the loops of structurally intact MOG, which should not be provided in a peptide ELISA, and indeed two studies failed to identify these epitopes in an ELISA assay [Xu *et al.* 2012, Haase *et al.* 2001]. Another study reported that linear epitopes aa 37–48 and aa 42–53 are immunodominant in a peptide ELISA assay, but these peptides were also recognized by controls at a lower frequency [Khalil *et al.* 2006]. The donors assessed in [Khalil *et al.* 2006] were adult MS patients, who rarely have IgG against conformationally intact MOG. In addition, because a secondary antibody recognizing IgG, IgA, and IgM was used in that study, it is likely that mainly low-affinity IgM was detected.

30 Relevance of MOG-glycosylation on recognition by human antibodies

To study the potential relevance of MOG-glycosylation in this study, the N31D mutant [O'Connor *et al.* 2007] was used. This mutation completely abolished N-glycosylation of MOG, indicating that in our MOG constructs N31 is the only used N-glycosylation site. A second potential glycosylation site N52, which lacks the consensus N-glycosylation sequence N-!P-[S|T], was found in mouse brain by tandem mass spectrometry [Zielinska *et al.* 2010]. This site was not considered a high-confidence glycosylation site [Zielinska *et al.* 2010] and it was not used to glycosylate MOG in HeLa cells in this study. In this study, unglycosylated MOG was recognized well by all human anti-MOG antibodies, in agreement with [O'Connor *et al.* 2007]. A subgroup of 8 in 111 sera even showed increased reactivity to unglycosylated MOG, which might be due to the better accessibility of MOG lacking the polycarbohydrate chain at its upper, very exposed edge of its extracellular domain. This effect is reminiscent of observations made in HIV, in which deglycosylation of the

HIV envelope glycoprotein gp120 led to increased recognition by neutralizing antibodies [Koch *et al.* 2003]. It will be of interest to analyze the glycosylation state of MOG in healthy and patient brain.

31 Increased recognition of MOG mutant H103A/S104E

In addition to unglycosylated MOG, other mutated variants of MOG were also recognized at least twice as good as hMOG: 17 of 111 sera recognized H103A/S104E better, and 6 of 111 recognized P42S better than hMOG. Mutation of serine to glutamic acid, as in the H103A/S104E mutant is used experimentally to mimic phosphorylation, a strategy called “pseudo-phosphorylation” [Xiao *et al.* 2009]. It is possible that these antibodies are generated against phosphorylated MOG. NetPhos 2.0 [Blom *et al.* 1999] was used to predict phosphorylation sites on hMOG and found S104 to be a likely site for phosphorylation, with a score of 0.994. Further experiments are required to confirm whether MOG in the human CNS is indeed phosphorylated at S104 or other positions. Some post-translational modifications have been shown to differ in patient brain, e.g. about 25% of the MBP molecules in healthy brain are citrullinated; this proportion can be up to 45% in MS patients and even 70% in Marburg’s disease [Lolli *et al.* 2006].

32 Temporal stability of epitope recognition

Although patients, in particular with ADEM, only show a transient IgG response to MOG, others (in particular with MS) tend to have a persisting antibody response to MOG [Di Pauli *et al.* 2011, Proebstel *et al.* 2011]. It was analyzed whether there was intramolecular epitope spreading of anti-MOG antibodies. Interestingly, the recognized epitopes remained constant. This was seen not only in patients with ADEM who rapidly

lose their anti-MOG antibodies, but also in pediatric patients with MS and CRION who have anti-MOG antibodies persisting for years. Hence, for MOG-antibodies there is neither intramolecular epitope spreading nor epitope loss. Autoantibody epitope spreading has been reported for a number of autoimmune targets, among them anti-AChR antibodies in myasthenia gravis [Vincent *et al.* 1994], anti-mitochondrial antibodies in primary biliary cirrhosis [Mori *et al.* 2012], and anti-citrullinated protein antibodies in rheumatoid arthritis [Sokolove *et al.* 2012]. Further experiments could analyze intermolecular epitope spreading using purified anti-MOG antibodies to screen CNS proteins or other proteins for cross-reactivity.

33 Stable IgG response upon vaccination in children rapidly losing anti-MOG IgG response

The maintenance of serum IgG is crucial for our ability to fight pathogens [Amanna *et al.* 2007]. The persistence of serum IgG is based on long-lived plasma cells that find a survival niche in the bone marrow or inflamed tissue [Manz *et al.* 2005]. It was of interest to examine whether those patients with a rapid decline of anti-MOG IgG were still able to mount a persisting IgG response to other antigens. As expected, patients, who rapidly lost their anti-MOG IgG, were still able to mount a persisting IgG response against two pathogens: measles and rubella virus. This finding shows that these patients do not have a general inability to generate long-lived plasma cells. Instead, it suggests that the IgG secreting cells generated during their anti-MOG response are less competent to seed the survival niches than are plasma cells generated after vaccination.

34 Therapeutic consequences

The identification of precise epitopes of autoantibodies can provide the basis for an antigen specific depletion of relevant B cells. A proof of concept for such an antigen specific therapy has recently been obtained in an animal model of diabetes [Henry *et al.* 2012]. This group used a mAb binding to insulin reactive B-cells to selectively deplete these. For this approach, it is important to know the epitope recognized by the autoreactive B-cells, as the applied mAb has to recognize a distinct epitope.

Many observations support the application of anti-CD20 treatment in NMO patients with anti-AQP4 antibodies [Pellkofer *et al.* 2011]. In contrast, IFN β is not a suitable treatment for many NMO patients, since it may worsen the disease [Palace *et al.* 2010]. This might be due to the induction of the B-cell survival factor BAFF by IFN β [Krumbholz *et al.* 2008]. Up to now there are no reports about IFN β treatment in anti-MOG positive patients. It seems plausible that patients with anti-MOG antibodies rather benefit from plasma exchange or a B-cell-directed therapy. The rapid decline of anti-MOG antibodies in ADEM patients [Proebstel *et al.* 2011] suggests that in these patients the antibodies are derived from short-lived plasma cells. For this reason, a reduction of anti-MOG antibodies after B-cell-directed therapy would be expected in these patients.

Bibliography

- [Aktas *et al.* 2010] Aktas, O., Kiz̄oery, P., Kieseier, B., Hartung, H.-P. Fingolimod is a potential novel therapy for multiple sclerosis. *Nat. Rev. Neurol.*, Jul 2010. 6(7):373–382.
- [Amanna *et al.* 2007] Amanna, I. J., Carlson, N. E., Slifka, M. K. Duration of humoral immunity to common viral and vaccine antigens. *N. Engl. J. Med.*, 2007. 357(19):1903–15.
- [Andrīoœau *et al.* 1998] Andrīoœau, K., Lemaire, C., Souvannavong, V., Adam, A. Induction of apoptosis by dexamethasone in the b cell lineage. *Immunopharmacology*, Jul 1998. 40(1):67–76.
- [Banwell *et al.* 2009] Banwell, B., Kennedy, J., Sadovnick, D., Arnold, D., Magalhaes, S., Wambara, K., Connolly, M., Yager, J., Mah, J., Shah, N., Sebire, G., Meaney, B., Dilenge, M., Lortie, A., Whiting, S., Doja, A., Levin, S., MacDonald, E., Meek, D., Wood, E., Lowry, N., Buckley, D., Yim, C., Awuku, M., Guimond, C., Cooper, P., Grand’Maison, F., Baird, J., Bhan, V., Bar-Or, A. Incidence of acquired demyelination of the cns in canadian children. *Neurology*, 2009. 72(3):232–239.

- [Bennett *et al.* 2009] Bennett, J., Lam, C., Kalluri, S., Saikali, P., Bautista, K., Dupree, C., Glogowska, M., Case, D., Antel, J., Owens, G., Gilden, D., Nessler, S., Stadelmann, C., Hemmer, B. Intrathecal pathogenic anti-aquaporin-4 antibodies in early neuromyelitis optica. *Ann. Neurol.*, 2009. 66(5):617–629.
- [Blom *et al.* 1999] Blom, N., Gammeltoft, S., Brunak, S. Sequence and structure-based prediction of eukaryotic protein phosphorylation sites. *J. Mol. Biol.*, 1999. 294(5):1351–62.
- [Bradl *et al.* 2009] Bradl, M., Misu, T., Takahashi, T., Watanabe, M., Mader, S., Reindl, M., Adzemovic, M., Bauer, J., Berger, T., Fujihara, K., Itoyama, Y., Lassmann, H. Neuromyelitis optica: pathogenicity of patient immunoglobulin in vivo. *Ann. Neurol.*, 2009. 66(5):630–643.
- [Brehm *et al.* 1999] Brehm, U., Piddlesden, S., Gardinier, M., Linington, C. Epitope specificity of demyelinating monoclonal autoantibodies directed against the human myelin oligodendrocyte glycoprotein (mog). *J. Neuroimmunol.*, 1999. 97(1-2):9–15.
- [Breithaupt *et al.* 2003] Breithaupt, C., Schubart, A., Zander, H., Skerra, A., Huber, R., Linington, C., Jacob, U. Structural insights into the antigenicity of myelin oligodendrocyte glycoprotein. *Proc. Natl. Acad. Sci. U.S.A.*, 2003. 100(16):9446–9451.
- [Breithaupt *et al.* 2008] Breithaupt, C., Schafer, B., Pellkofer, H., Huber, R., Linington, C., Jacob, U. Demyelinating myelin oligodendrocyte glycoprotein-specific autoantibody response is focused on one

- dominant conformational epitope region in rodents. *J. Immunol.*, 2008. 181(2):1255–1263.
- [Brilot *et al.* 2009] Brilot, F., Dale, R., Selter, R., Grummel, V., Kalluri, S., Aslam, M., Busch, V., Zhou, D., Cepok, S., Hemmer, B. Antibodies to native myelin oligodendrocyte glycoprotein in children with inflammatory demyelinating central nervous system disease. *Ann. Neurol.*, 2009. 66(6):833–842.
- [Brunner *et al.* 1989] Brunner, C., Lassmann, H., Waehneltd, T., Matthieu, J., Lington, C. Differential ultrastructural localization of myelin basic protein, myelin/oligodendroglial glycoprotein, and 2',3'-cyclic nucleotide 3'-phosphodiesterase in the cns of adult rats. *J. Neurochem.*, 1989. 52(1):296–304.
- [Bjœdingen *et al.* 2002] von Bjœdingen, H., Hauser, S., Fuhrmann, A., Nabavi, C., Lee, J., Genain, C. Molecular characterization of antibody specificities against myelin/oligodendrocyte glycoprotein in autoimmune demyelination. *Proc. Natl. Acad. Sci. U.S.A.*, 2002. 99(12):8207–8212.
- [Bjœdingen *et al.* 2004] von Bjœdingen, H. C., Hauser, S. L., Ouallet, J. C., Tanuma, N., Menge, T., Genain, C. P. Frontline: Epitope recognition on the myelin/oligodendrocyte glycoprotein differentially influences disease phenotype and antibody effector functions in autoimmune demyelination. *Eur. J. Immunol.*, 2004. 34(8):2072–83.
- [Clements *et al.* 2003] Clements, C., Reid, H., Beddoe, T., Tynan, F., Perugini, M., Johns, T., Bernard, C., Rossjohn, J. The crystal struc-

- ture of myelin oligodendrocyte glycoprotein, a key autoantigen in multiple sclerosis. *Proc. Natl. Acad. Sci. U.S.A.*, 2003. 100(19):11059–11064.
- [Cong *et al.* 2011] Cong, H., Jiang, Y., Tien, P. Identification of the myelin oligodendrocyte glycoprotein as a cellular receptor for rubella virus. *J. Virol.*, Nov 2011. 85(21):11038–11047.
- [Delarasse *et al.* 2003] Delarasse, C., Daubas, P., Mars, L., Vizler, C., Litzemberger, T., Iglesias, A., Bauer, J., Della, G. B., Schubart, A., Decker, L., Dimitri, D., Roussel, G., Dierich, A., Amor, S., Dautigny, A., Liblau, R., Pham-Dinh, D. Myelin/oligodendrocyte glycoprotein-deficient (mog-deficient) mice reveal lack of immune tolerance to mog in wild-type mice. *J. Clin. Invest.*, 2003. 112(4):544–553.
- [Della Gaspera *et al.* 1998] Della Gaspera, B., Pham-Dinh, D., Roussel, G., Nussbaum, J., Dautigny, A. Membrane topology of the myelin/oligodendrocyte glycoprotein. *Eur. J. Biochem.*, 1998. 258(2):478–484.
- [Di Pauli *et al.* 2011] Di Pauli, F., Mader, S., Rostasy, K., Schanda, K., Bajer-Kornek, B., Ehling, R., Deisenhammer, F., Reindl, M., Berger, T. Temporal dynamics of anti-mog antibodies in cns demyelinating diseases. *Clin. Immunol.*, 2011. 138(3):247–254.
- [Fust *et al.* 2012] Fust, G., Uray, K., Bene, L., Hudecz, F., Karadi, I., Prohaszka, Z. Comparison of epitope specificity of anti-heat shock protein 60/65 igg type antibodies in the sera of healthy subjects,

- patients with coronary heart disease and inflammatory bowel disease. *Cell stress chaperon.*, 2012. 17(2):215–27.
- [Gardinier *et al.* 1993] Gardinier, M. V., Matthieu, J. M. Cloning and cdna sequence analysis of myelin/oligodendrocyte glycoprotein: a novel member of the immunoglobulin gene superfamily. *Schweiz. Arch. Neurol.*, 1993. 144(3):201–7.
- [Genain *et al.* 1995] Genain, C. P., Nguyen, M. H., Letvin, N. L., Pearl, R., Davis, R. L., Adelman, M., Lees, M. B., Linington, C., Hauser, S. L. Antibody facilitation of multiple sclerosis-like lesions in a non-human primate. *J. Clin. Invest.*, 1995. 96(6):2966–74.
- [Haase *et al.* 2001] Haase, C., Guggenmos, J., Brehm, U., Andersson, M., Olsson, T., Reindl, M., Schneidewind, J., Zettl, U., Heidenreich, F., Berger, T., Wekerle, H., Hohlfeld, R., Linington, C. The fine specificity of the myelin oligodendrocyte glycoprotein autoantibody response in patients with multiple sclerosis and normal healthy controls. *J. Neuroimmunol.*, 2001. 114(1-2):220–225.
- [Hauser *et al.* 2008] Hauser, S. L., Waubant, E., Arnold, D. L., Vollmer, T., Antel, J., Fox, R. J., Bar-Or, A., Panzara, M., Sarkar, N., Agarwal, S., Langer-Gould, A., Smith, C. H., Group, H. T. B-cell depletion with rituximab in relapsing-remitting multiple sclerosis. *N. Engl. J. Med.*, 2008. 358(7):676–88.
- [Henry *et al.* 2012] Henry, R. A., Kendall, P. L., Thomas, J. W. Autoantigen-specific b-cell depletion overcomes failed immune tolerance in type 1 diabetes. *Diabetes*, 2012. 61(8):2037–44.

- [Iorio *et al.* 2012] Iorio, R., Lennon, V. A. Neural antigen-specific autoimmune disorders. *Immunol. Rev.*, 2012. 248(1):104–21.
- [Jacob *et al.* 2013] Jacob, A., McKeon, A., Nakashima, I., Sato, D. K., Elson, L., Fujihara, K., de Seze, J. Current concept of neuromyelitis optica (nmo) and nmo spectrum disorders. *J. Neurol. Neurosurg. Psychiatry*, Aug 2013. 84(8):922–930.
- [Johns *et al.* 1997] Johns, T., Bernard, C. Binding of complement component clq to myelin oligodendrocyte glycoprotein: a novel mechanism for regulating cns inflammation. *Mol. Immunol.*, 1997. 34(1):33–38.
- [Kappos *et al.* 2011] Kappos, L., Li, D., Calabresi, P. A., O’Connor, P., Bar-Or, A., Barkhof, F., Yin, M., Leppert, D., Glanzman, R., Tinbergen, J., Hauser, S. L. Ocrelizumab in relapsing-remitting multiple sclerosis: a phase 2, randomised, placebo-controlled, multicentre trial. *Lancet*, Nov 2011. 378(9805):1779–1787.
- [Keegan *et al.* 2005] Keegan, M., Konig, F., McClelland, R., Bruck, W., Morales, Y., Bitsch, A., Panitch, H., Lassmann, H., Weinshenker, B., Rodriguez, M., Parisi, J., Lucchinetti, C. Relation between humoral pathological changes in multiple sclerosis and response to therapeutic plasma exchange. *Lancet*, 2005. 366(9485):579–582.
- [Khalil *et al.* 2006] Khalil, M., Reindl, M., Lutterotti, A., Kuenz, B., Ehling, R., Gneiss, C., Lackner, P., Deisenhammer, F., Berger, T. Epitope specificity of serum antibodies directed against the extracellular domain of myelin oligodendrocyte glycoprotein: Influence

- of relapses and immunomodulatory treatments. *J. Neuroimmunol.*, 2006. 174(1-2):147–56.
- [Kidd *et al.* 2003] Kidd, D., Burton, B., Plant, G. T., Graham, E. M. Chronic relapsing inflammatory optic neuropathy (crion). *Brain*, 2003. 126(Pt 2):276–84.
- [Kim *et al.* 2013] Kim, S. H., Kim, W., Huh, S. Y., Lee, K. Y., Jung, I. J., Kim, H. J. Clinical efficacy of plasmapheresis in patients with neuromyelitis optica spectrum disorder and effects on circulating anti-aquaporin-4 antibody levels. *J. Clin. Immunol.*, 2013. 9(1):36–42.
- [Kinoshita *et al.* 2009] Kinoshita, M., Nakatsuji, Y., Kimura, T., Moriya, M., Takata, K., Okuno, T., Kumanogoh, A., Kajiyama, K., Yoshikawa, H., Sakoda, S. Neuromyelitis optica: Passive transfer to rats by human immunoglobulin. *Biochem. Biophys. Res. Commun.*, 2009. 386(4):623–627.
- [Kitley *et al.* 2012] Kitley, J., Woodhall, M., Waters, P., Leite, M. I., Devenney, E., Craig, J., Palace, J., Vincent, A. Myelin-oligodendrocyte glycoprotein antibodies in adults with a neuromyelitis optica phenotype. *Neurology*, 2012. 79(12):1273–7.
- [Koch *et al.* 2003] Koch, M., Pancera, M., Kwong, P. D., Kolchinsky, P., Gruninger, C., Wang, L., Hendrickson, W. A., Sodroski, J., Wyatt, R. Structure-based, targeted deglycosylation of hiv-1 gp120 and effects on neutralization sensitivity and antibody recognition. *Virology*, 2003. 313(2):387–400.

- [Kroepfl *et al.* 1996] Kroepfl, J. F., Viise, L. R., Charron, A. J., Linington, C., Gardinier, M. V. Investigation of myelin/oligodendrocyte glycoprotein membrane topology. *J. Neurochem.*, 1996. 67(5):2219–22.
- [Krumbholz *et al.* 2008] Krumbholz, M., Faber, H., Steinmeyer, F., Hoffmann, L., Kumpfel, T., Pellkofer, H., Derfuss, T., Ionescu, C., Starck, M., Hafner, C., Hohlfeld, R., Meinl, E. Interferon-beta increases baffle levels in multiple sclerosis: implications for b cell autoimmunity. *Brain*, 2008. 131(Pt 6):1455–1463.
- [Krumbholz *et al.* 2012] Krumbholz, M., Derfuss, T., Hohlfeld, R., Meinl, E. B cells and antibodies in multiple sclerosis pathogenesis and therapy. *Nat. Rev. Neurol.*, 2012. 8(11):613–23.
- [Lalive *et al.* 2011] Lalive, P., Hausler, M., Maurey, H., Mikaeloff, Y., Tardieu, M., Wiendl, H., Schroeter, M., Hartung, H., Kieseier, B., Menge, T. Highly reactive anti-myelin oligodendrocyte glycoprotein antibodies differentiate demyelinating diseases from viral encephalitis in children. *Mult.Scler.*, 2011. 17(3):297–302.
- [Lancaster *et al.* 2012] Lancaster, E., Dalmau, J. Neuronal autoantigen–pathogenesis, associated disorders and antibody testing. *Nat. Rev. Neurol.*, 2012. 8(7):380–90.
- [Lennon *et al.* 2004] Lennon, V. A., Wingerchuk, D. M., Kryzer, T. J., Pittock, S. J., Lucchinetti, C. F., Fujihara, K., Nakashima, I., Weinshenker, B. G. A serum autoantibody marker of neuromyelitis optica: distinction from multiple sclerosis. *Lancet*, 2004. 364(9451):2106–12.

- [Linnington *et al.* 1988] Linnington, C., Bradl, M., Lassmann, H., Brunner, C., Vass, K. Augmentation of demyelination in rat acute allergic encephalomyelitis by circulating mouse monoclonal antibodies directed against a myelin/oligodendrocyte glycoprotein. *Am. J. Pathol.*, 1988. 130(3):443–454.
- [Linnington *et al.* 1984] Linnington, C., Webb, M., Woodhams, P. A novel myelin-associated glycoprotein defined by a mouse monoclonal antibody. *J. Neuroimmunol.*, 1984. 6(6):387–396.
- [Litzenburger *et al.* 1998] Litzenburger, T., Fassler, R., Bauer, J., Lassmann, H., Linnington, C., Wekerle, H., Iglesias, A. B lymphocytes producing demyelinating autoantibodies: development and function in gene-targeted transgenic mice. *J. Exp. Med.*, 1998. 188(1):169–180.
- [Lolli *et al.* 2006] Lolli, F., Rovero, P., Chelli, M., Papini, A. M. Toward biomarkers in multiple sclerosis: new advances. *Exp. Rev. Neuroth.*, May 2006. 6(5):781–794.
- [Luo *et al.* 2009] Luo, J., Taylor, P., Losen, M., de Baets, M. H., Shelton, G. D., Lindstrom, J. Main immunogenic region structure promotes binding of conformation-dependent myasthenia gravis autoantibodies, nicotinic acetylcholine receptor conformation maturation, and agonist sensitivity. *J. Neurosci.*, 2009. 29(44):13898–908.
- [Mader *et al.* 2011] Mader, S., Gredler, V., Schanda, K., Rostasy, K., Dujmovic, I., Pfaller, K., Lutterotti, A., Jarius, S., Di, P. F., Kuenz, B., Ehling, R., Hegen, H., Deisenhammer, F., Aboul-Enein, F.,

- Storch, M., Koson, P., Drulovic, J., Kristoferitsch, W., Berger, T., Reindl, M. Complement activating antibodies to myelin oligodendrocyte glycoprotein in neuromyelitis optica and related disorders. *J. Neuroinflamm.*, 2011. 8:184.
- [Magana *et al.* 2011] Magana, S. M., Keegan, B. M., Weinshenker, B. G., Erickson, B. J., Pittock, S. J., Lennon, V. A., Rodriguez, M., Thomsen, K., Weigand, S., Mandrekar, J., Linbo, L., Lucchinetti, C. F. Beneficial plasma exchange response in central nervous system inflammatory demyelination. *Arch. Neuro.*, 2011. 68(7):870–8.
- [Manz *et al.* 2005] Manz, R. A., Hauser, A. E., Hiepe, F., Radbruch, A. Maintenance of serum antibody levels. *Ann. Rev. Immunol.*, 2005. 23:367–86.
- [Marta *et al.* 2005] Marta, C., Oliver, A., Sweet, R., Pfeiffer, S., Ruddle, N. Pathogenic myelin oligodendrocyte glycoprotein antibodies recognize glycosylated epitopes and perturb oligodendrocyte physiology. *Proc. Natl. Acad. Sci. U.S.A.*, 2005. 102(39):13992–13997.
- [Mayer *et al.* 2012] Mayer, M. C., Meinl, E. Glycoproteins as targets of autoantibodies in CNS inflammation: Mog and more. *Ther. Adv. Neurol. Disord.*, 2012. 5(3):147–59.
- [Mayer *et al.* 2013] Mayer, M. C., Breithaupt, C., Reindl, M., Schanda, K., Rostasy, K., Berger, T., Dale, R., Brilot, F., Olsson, T., Jenne, D., Proebstel, A. K., Dornmair, K., Wekerle, H., Hohlfeld, R., Banwell, B., Bar-Or, A., Meinl, E. Distinction and temporal stability of conformational epitopes on myelin oligodendro-

- cyte glycoprotein recognized by patients with different inflammatory central nervous system diseases. *J. Immunol.*, 2013. 191(7):3594–3604.
- [McLaughlin *et al.* 2009] McLaughlin, K., Chitnis, T., Newcombe, J., Franz, B., Kennedy, J., McArdel, S., Kuhle, J., Kappos, L., Rostasy, K., Pohl, D., Gagne, D., Ness, J., Tenenbaum, S., O'Connor, K., Viglietta, V., Wong, S., Tavakoli, N., de, S. J., Idrissova, Z., Khoury, S., Bar-Or, A., Hafler, D., Banwell, B., Wucherpfennig, K. Age-dependent b cell autoimmunity to a myelin surface antigen in pediatric multiple sclerosis. *J. Immunol.*, 2009. 183(6):4067–4076.
- [Mori *et al.* 2012] Mori, T., Ohira, H., Kuroda, M., Kato, M., Yamaguchi, Y., Kochi, H. Characterization of autoantibodies against the e1alpha subunit of branched-chain 2-oxoacid dehydrogenase in patients with primary biliary cirrhosis. *Int. J. Hepatol.*, 2012. 2012:369740.
- [O'Connor *et al.* 2007] O'Connor, K., McLaughlin, K., De Jager, P., Chitnis, T., Bettelli, E., Xu, C., Robinson, W., Cherry, S., Bar-Or, A., Banwell, B., Fukaura, H., Fukazawa, T., Tenenbaum, S., Wong, S., Tavakoli, N., Idrissova, Z., Viglietta, V., Rostasy, K., Pohl, D., Dale, R., Freedman, M., Steinman, L., Buckle, G., Kuchroo, V., Hafler, D., Wucherpfennig, K. Self-antigen tetramers discriminate between myelin autoantibodies to native or denatured protein. *Nat. Med.*, 2007. 13(2):211–217.

- [Palace *et al.* 2010] Palace, J., Leite, M., Nairne, A., Vincent, A. Interferon beta treatment in neuromyelitis optica: increase in relapses and aquaporin 4 antibody titers. *Arch. Neurol.*, 2010. 67(8):1016–1017.
- [Pellkofer *et al.* 2011] Pellkofer, H., Krumbholz, M., Berthele, A., Hemmer, B., Gerdes, L., Havla, J., Bittner, R., Canis, M., Meinl, E., Hohlfeld, R., Kuempfel, T. Long-term follow-up of patients with neuromyelitis optica after repeated therapy with rituximab. *Neurology*, 2011. 76(15):1310–1315.
- [Piddlesden *et al.* 1993] Piddlesden, S., Lassmann, H., Zimprich, F., Morgan, B., Lington, C. The demyelinating potential of antibodies to myelin oligodendrocyte glycoprotein is related to their ability to fix complement. *Am. J. Pathol.*, 1993. 143(2):555–564.
- [Poser *et al.* 2007] Poser, C., Brinar, V. Disseminated encephalomyelitis and multiple sclerosis: two different diseases - a critical review. *Acta Neurol. Scand.*, 2007. 116(4):201–206.
- [Proebstel *et al.* 2011] Proebstel, A., Dornmair, K., Bittner, R., Sperl, P., Jenne, D., Magalhaes, S., Villalobos, A., Breithaupt, C., Weissert, R., Jacob, U., Krumbholz, M., Kuempfel, T., Blaschek, A., Stark, W., Gartner, J., Pohl, D., Rostasy, K., Weber, F., Forne, I., Khademi, M., Olsson, T., Brilot, F., Tantsis, E., Dale, R., Wekerle, H., Hohlfeld, R., Banwell, B., Bar-Or, A., Meinl, E., Derfuss, T. Antibodies to mog are transient in childhood acute disseminated encephalomyelitis. *Neurology*, 2011. 77(6):580–588.

- [Quintana *et al.* 2008] Quintana, F., Farez, M., Viglietta, V., Iglesias, A., Merbl, Y., Izquierdo, G., Lucas, M., Basso, A., Khoury, S., Lucchinetti, C., Cohen, I., Weiner, H. Antigen microarrays identify unique serum autoantibody signatures in clinical and pathologic subtypes of multiple sclerosis. *Proc. Natl. Acad. Sci. U.S.A.*, 2008. 105(48):18889–18894.
- [Ramaraj *et al.* 2012] Ramaraj, T., Angel, T., Dratz, E. A., Jesaitis, A. J., Mumey, B. Antigen-antibody interface properties: composition, residue interactions, and features of 53 non-redundant structures. *Biochim. Biophys. Acta*, 2012. 1824(3):520–32.
- [Ransohoff *et al.* 2012] Ransohoff, R. M., Engelhardt, B. The anatomical and cellular basis of immune surveillance in the central nervous system. *Nat Rev Immunol*, Sep 2012. 12(9):623–635.
- [Reindl *et al.* 2013] Reindl, M., Pauli, F. D., Rostj csy, K., Berger, T. The spectrum of mog autoantibody-associated demyelinating diseases. *Nat. Rev. Neurol.*, Aug 2013. 9(8):455–461.
- [Rostasy *et al.* 2012] Rostasy, K., Mader, S., Schanda, K., Huppke, P., Gartner, J., Kraus, V., Karenfort, M., Tibussek, D., Blaschek, A., Bajer-Kornek, B., Leitz, S., Schimmel, M., Di Pauli, F., Berger, T., Reindl, M. Anti-myelin oligodendrocyte glycoprotein antibodies in pediatric patients with optic neuritis. *Arch. Neurol.*, 2012. 69(6):752–6.
- [Rostasy *et al.* 2013] Rostasy, K., Mader, S., Hennes, E., Schanda, K., Gredler, V., Guenther, A., Blaschek, A., Korenke, C., Pritsch, M., Pohl, D., Maier, O., Kuchukhidze, G., Brunner-Krainz, M., Berger,

- T., Reindl, M. Persisting myelin oligodendrocyte glycoprotein antibodies in aquaporin-4 antibody negative pediatric neuromyelitis optica. *Mult. Scler.*, 2013. 19(8):1052–9.
- [Saadoun *et al.* 2010] Saadoun, S., Waters, P., Bell, B. A., Vincent, A., Verkman, A. S., Papadopoulos, M. C. Intra-cerebral injection of neuromyelitis optica immunoglobulin g and human complement produces neuromyelitis optica lesions in mice. *Brain*, 2010. 133(Pt 2):349–61.
- [Saadoun *et al.* 2011] Saadoun, S., Waters, P., Macdonald, C., Bridges, L., Bell, B., Vincent, A., Verkman, A., Papadopoulos, M. T cell deficiency does not reduce lesions in mice produced by intracerebral injection of nmo-igg and complement. *J. Neuroimmunol.*, 2011. 235(1-2):27–32.
- [Schluesener *et al.* 1987] Schluesener, H., Sobel, R., Linington, C., Weiner, H. A monoclonal antibody against a myelin oligodendrocyte glycoprotein induces relapses and demyelination in central nervous system autoimmune disease. *J. Immunol.*, 1987. 139(12):4016–4021.
- [Schwede *et al.* 2003] Schwede, T., Kopp, J., Guex, N., Peitsch, M. C. Swiss-model: An automated protein homology-modeling server. *Nucleic Acids Res.*, 2003. 31(13):3381–5.
- [Sokolove *et al.* 2012] Sokolove, J., Bromberg, R., Deane, K. D., Lahey, L. J., Derber, L. A., Chandra, P. E., Edison, J. D., Gilliland, W. R., Tibshirani, R. J., Norris, J. M., Holers, V. M., Robinson, W. H. Autoantibody epitope spreading in the pre-clinical phase pre-

- dicts progression to rheumatoid arthritis. *PloS one*, 2012. 7(5):e35296.
- [Sospedra *et al.* 2005] Sospedra, M., Martin, R. Immunology of multiple sclerosis. *Ann. Rev. Immunol.*, 2005. 23:683–747.
- [Srivastava *et al.* 2012] Srivastava, R., Aslam, M., Kalluri, S. R., Schirmer, L., Buck, D., Tackenberg, B., Rothhammer, V., Chan, A., Gold, R., Berthele, A., Bennett, J. L., Korn, T., Hemmer, B. Potassium channel kir4.1 as an immune target in multiple sclerosis. *N. Engl. J. Med.*, 2012. 367(2):115–23.
- [Tenenbaum *et al.* 2002] Tenenbaum, S., Chamoles, N., Fejerman, N. Acute disseminated encephalomyelitis: a long-term follow-up study of 84 pediatric patients. *Neurology*, 2002. 59(8):1224–1231.
- [Thornton *et al.* 1986] Thornton, J. M., Edwards, M. S., Taylor, W. R., Barlow, D. J. Location of 'continuous' antigenic determinants in the protruding regions of proteins. *EMBO J.*, 1986. 5(2):409–13.
- [Tsiakalos *et al.* 2011] Tsiakalos, A., Routsias, J. G., Kordossis, T., Moutsopoulos, H. M., Tzioufas, A. G., Sipsas, N. V. Fine epitope specificity of anti-erythropoietin antibodies reveals molecular mimicry with hiv-1 p17 protein: a pathogenetic mechanism for hiv-1-related anemia. *J. Infect. Dis.*, 2011. 204(6):902–11.
- [Tzartos *et al.* 1982] Tzartos, S. J., Seybold, M. E., Lindstrom, J. M. Specificities of antibodies to acetylcholine receptors in sera from myasthenia gravis patients measured by monoclonal antibodies. *Proc. Natl. Acad. Sci. U.S.A.*, 1982. 79(1):188–92.

- [Vincent *et al.* 1994] Vincent, A., Jacobson, L., Shillito, P. Response to human acetylcholine receptor alpha 138-199: determinant spreading initiates autoimmunity to self-antigen in rabbits. *Immunol. Lett.*, 1994. 39(3):269–75.
- [Vincent *et al.* 2011] Vincent, A., Bien, C. G., Irani, S. R., Waters, P. Autoantibodies associated with diseases of the CNS: new developments and future challenges. *Lancet Neurol.*, 2011. 10(8):759–72.
- [Waubant *et al.* 2009] Waubant, E., Chabas, D., Okuda, D., Glenn, O., Mowry, E., Henry, R., Strober, J., Soares, B., Wintermark, M., Pelletier, D. Difference in disease burden and activity in pediatric patients on brain magnetic resonance imaging at time of multiple sclerosis onset vs adults. *Arch. Neurol.*, 2009. 66(8):967–971.
- [Weinshenker *et al.* 2006] Weinshenker, B., Wingerchuk, D., Pittock, S., Lucchinetti, C., Lennon, V. NMO-IGG: a specific biomarker for neuromyelitis optica. *Dis. Markers*, 2006. 22(4):197–206.
- [Xiao *et al.* 1991] Xiao, B., Linington, C., Link, H. Antibodies to myelin-oligodendrocyte glycoprotein in cerebrospinal fluid from patients with multiple sclerosis and controls. *J. Neuroimmunol.*, 1991. 31(2):91–96.
- [Xiao *et al.* 2009] Xiao, Q., Yu, K., Cui, Y. Y., Hartzell, H. C. Dysregulation of human bestrophin-1 by ceramide-induced dephosphorylation. *J. Physiol.*, 2009. 587(Pt 18):4379–91.
- [Xu *et al.* 2012] Xu, Y., Zhang, Y., Liu, C. Y., Peng, B., Wang, J. M., Zhang, X. J., Li, H. F., Cui, L. Y. Serum antibodies to 25 myelin

oligodendrocyte glycoprotein epitopes in multiple sclerosis and neuromyelitis optica: clinical value for diagnosis and disease activity. *Chin. med. J.*, 2012. 125(18):3207–10.

[Zhou *et al.* 2006]

Zhou, D., Srivastava, R., Nessler, S., Grummel, V., Sommer, N., Bruck, W., Hartung, H., Stadelmann, C., Hemmer, B. Identification of a pathogenic antibody response to native myelin oligodendrocyte glycoprotein in multiple sclerosis. *Proc. Natl. Acad. Sci. U.S.A.*, 2006. 103(50):19057–19062.

[Zielinska *et al.* 2010]

Zielinska, D. F., Gnad, F., Wisniewski, J. R., Mann, M. Precision mapping of an in vivo n-glycoproteome reveals rigid topological and sequence constraints. *Cell*, 2010. 141(5):897–907.